Electronic Supplementary Material (ESI) for Chemical Science.

Investigating pyridazine and phthalazine exchange in a series of iridium complexes in order to define their role in the catalytic transfer of magnetisation from *para*hydrogen

Kate M. Appleby, Ryan E. Mewis, Alexandra M. Olaru, Gary G. R. Green, Ian J. S. Fairlamb and Simon B. Duckett*

Centre for Hyperpolarisation in Magnetic Resonance, Department of Chemistry, University of York, York, YO10 5DD, UK.

Contents

Supplementary Data

1. Characterisation data

[Ir(COD)(IMes)(pdz)]Cl (2a)

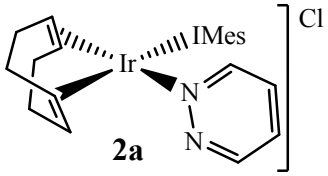

2a

^{1}H NMR (500 MHz, methanol-d4): 9.08 (d, 1H, J_{HH} = 4Hz, IrNC***H***), 7.88 (d, 1H, J_{HH} = 5 Hz, IrNNC***H***), 7.70 (m, 1H, IrNCHC***H***), 7.51 (m, 1H, IrNNCHC***H***), 7.43 (s, 2H, IrCNC***H***), 7.23 (s, 2H, NCC(CH_3)C***H***), 6.94 (s, 2H, NCC(CH_3)C***H***), 3.70 (s, 2H, IrCH), 3.29 (m, 2H, IrCH), 2.45 (s, 6H, NCC(CH_3)CHC(C***H₃***)), 2.37 (s, 6H, NCC(C***H₃***)), 2.00 (m, 4H, IrCHC***H₂***), 1.90 (s, 6H, NCC(C***H₃***)), 1.67 (m, 4H, IrCHC***H₂***). ^{13}C NMR (400 MHz, methanol-d4): 173 (s, Ir***C***N), 155 (s, IrNN***C***H), 153 (s, IrN***C***H), 148 (s, NC***C***(CH_3)), 140 (s, NCC(CH_3)CH***C***(CH_3)), 136 (s, N***C***C(CH_3)), 135 (s, NC***C***(CH_3)), 131 (s, IrNNCH***C***H), 129 (s, NCC(CH_3)***C***H), 127 s, (IrNCH***C***H), 125 (s, IrCN***C***H), 81 (s, Ir***C***H), 65 (s, Ir***C***H), 32 (s, IrCHCH_2), 29 (s, IrCHCH_2), 20 (s, NCC(CH_3)CHC(***C***H_3)), 17 (s, NCC(***C***H_3)). ^{15}N NMR (500 MHz, methanol-d_4): 386.1 (Ir***N***), 311.8 (IrN***N***), 195.4 (IrC***N***). ESI (MS): 685.4 [M-Cl], 605.4 [M-Cl-pdz].

[Ir(COD)(IMes)(phth)]Cl (2b)

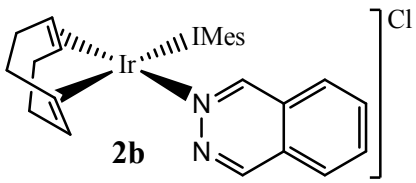

2b

^{1}H NMR (400 MHz, methanol-d_4): 9.55 (s, 1H, IrNC***H***), 8.37 (s, 1H, IrNNC***H***), 8.22-8.18 (m, 3H, IrNNCHCC***H***C***H***C***H***), 7.86 (d, 1H, *J* = 6.6, IrNCHCC***H***), 7.40 (s, 2H, IrCNC***H***), 7.27 (s, 2H, NCC(CH_3)C***H***), 6.61 (s, 2H, NC(CH_3)C***H***), 3.71 (s (br), 2H, IrC***H***), 3.40 (m, 2H, IrC***H***), 2.43 (s, 6H, NCC(CH_3)CHC(C***H₃***)), 2.40 (s, 6H, NCC(C***H₃***)), 2.05 (m, 4H, IrCHCH_2), 1.91 (m, 4H, IrCHC***H₂***)), 1.70 (s, 6H, NCC(C***H₃***)). ^{13}C NMR (400 MHz, methanol-d_4): 172 (s, Ir***C***N), 155 (s, IrNN***C***H), 152 (s, IrN***C***H), 139 (s, NCC(CH_3)CH***C***(CH_3)), 136 (s, N***C***C(CH_3)), 135 (s, IrNNCHC***C***H***C***H***C***H), 129 (s, NCC(CH_3)***C***H), 128 (s, NCC(CH_3)***C***H), 128 (s, IrNNCH***C***), 127 (s, IrNNCHC***C***H***C***H***C***H), 127 (s, IrNCHCC***H***), 125 (s, IrNCH***C***), 125 (s, IrCN***C***H), 81 (s, Ir***C***H), 29 (s, IrCH***C***H_2), 20 (s, NCC(CH_3)CHC(***C***H_3)), 17 (NC***C***(CH_3)). ^{15}N NMR (500 MHz, methanol-d_4): 386.0 (Ir***N***), 311.5 (IrN***N***), 195.2 (IrC***N***). ESI (MS): 735.4 [M-Cl], 605.4 [M-Cl-phth].

[Ir(COD)(H)$_2$(IMes)(pdz)]Cl (3a)

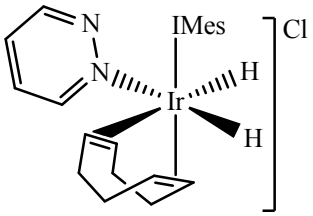

3a

^{1}H NMR (methanol-d_4, 500 MHz): 9.05 (d, J = 4.8, 1H, IrNNC***H***), 9.02 (d, J = 5.5, 1H, IrNC***H***), 7.90 (d.d, J = 8.3, 5.1, 1H, IrNNCHC***H***), 7.62 (d.d, J = 8.3, 5.1, 1H, IrNCHC***H***), 7.36 (s, 2H, IrCNC***H***), 7.03 (s, 2H, NCC(CH$_3$)C***H***), 7.00 (s, 2H, NCC(CH$_3$)C***H***), 5.09 (m (br), 1H, IrC***H***) 5.02 (m (br), 1H, IrC***H***), 4.45 (m (br), 1H, IrC***H***), 3.74 (m (br), 1H, IrC***H***), 2.54 (m (br), 1H, IrCHC***H$_2$***), 2.39 (s, 6H, NCC(CH$_3$)CHC(C***H$_3$***)), 2.23 (m (br), 1H, IrCHC***H$_2$***), 2.19 (s, 6H, NCC(C***H$_3$***)), 2.00 (m (br), 1H, IrCHC***H$_2$***), 1.90 (m (br), 2H, IrCHC***H$_2$***), 1.81 (s, 6H, NCC(C***H$_3$***)), 1.75 (m (br), 1H, IrCHC***H$_2$***), 1.65 (m (br), 1H, IrCHC***H$_2$***), 1.25 (m (br), 1H, IrCHC***H$_2$***), -13.84 (d, J = 3.8, 1H, ***H***IrCH), -17.69 (d, J = 3.8, 1H, ***H***IrN). ^{13}C NMR (methanol-d_4, 400 MHz): 163.1 (s, IrNN***C***H), 154.2 (s, Ir***C***N), 153.12 (IrN***C***H), 139.6 (s, NCC(CH$_3$)CH***C***(CH$_3$)), 136.6 (s, NC***C***(CH$_3$)), 135.4 (s, N***C***C(CH$_3$)), 131.2 (s, IrNCH***C***H), 129.2 (s, NCC(CH$_3$)***C***H), 128.8 (s, NCC(CH$_3$)***C***H), 128.1 (s, IrNNCH***C***H), 124.1 (IrCN***C***H), 97.7 (s, Ir***C***H), 95.1 (s, Ir***C***H), 82.6 (s, Ir***C***H), 79.0 (s, Ir***C***H), 34.4 (s, IrCH***C***H$_2$), 30.8 (s, IrCH***C***H$_2$), 28.3 (s, IrCH***C***H$_2$), 27.8 (s, IrCH***C***H$_2$), 19.7 (s, NCC(CH$_3$)CHC(***C***H$_3$)), 17.6 (s, NCC(***C***H$_3$)), 16.6 (s, NCC(CH$_3$)). ^{15}N NMR (methanol-d_4, 500 MHz): 400.1 (IrN***N***), 294.3 (Ir***N***N), 197.8 (IrC***N***).

[Ir(COD)(H)$_2$(IMes)(phth)]Cl (3b)

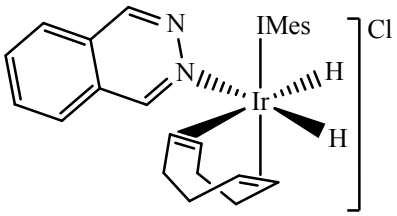

3b

^{1}H NMR (methanol-d_4, 500 MHz): 9.52 (s, 1H, IrNNC***H***), 9.45 (s, 1H, IrNC***H***), 8.31 (d, J = 7.9, 1H, IrNNCHCC***H***), 8.27 (t.d, J = 7.5, 1.0, 1H, IrNCHCCHC***H***), 8.21 (t.d, J = 7.5, 1.0, 1H, IrNNCHCCHC***H***), 8.03 (d, J = 8.0, 1H, IrNCHCC***H***), 7.32 (s, 2H, IrCNC***H***), 6.99 (s, 2H, NCC(CH$_3$)C***H***), 6.76 (s, 2H, NCC(CH$_3$)C***H***), 5.23 (m, 1H, IrC***H***) 5.18 (m, 1H, IrC***H***), 4.33 (m, 1H, IrC***H***), 3.85 (t.d, J = 8.4, 3.9, 1H, IrC***H***), 2.76 (m (br), 1H, IrCHC***H$_2$***), 2.34 (s, 6H, NCC(CH$_3$)CHC(C***H$_3$***)), 2.26 (s, 6H, NCC(C***H$_3$***)), 2.01 (m (br), 1H, IrCHC***H$_2$***), 1.90 (m (br), 1H, IrCHC***H$_2$***), 1.74 (m (br), 3H, IrCHC***H$_2$***), 1.62 (s, 6H, NCC(C***H$_3$***)), 1.38 (m (br), 2H, IrCHC***H$_2$***), -13.87 (d, J = 4.0, 1H, ***H***IrCH), -17.55 (d, J = 5.1, 1H, ***H***IrN). ^{13}C NMR (methanol-d_4, 400 MHz): 162.8 (s, IrN***C***H), 154.2 (s, Ir***C***N), 153.0 (IrNN***C***H), 139.5 (s, NC***C***(CH$_3$)) 136.8 (s, N***C***C(CH$_3$)), 135.4 (s, NCC(CH$_3$)CH***C***(CH$_3$)), 135.1 (s, IrNCHCCH***C***H***C***H), 129.2 (s, NCC(CH$_3$)***C***H), 128.7 (s, IrNNCH***C***), 128.4 (s, NCC(CH$_3$)***C***H), 127.0 (s, IrNCHC***C***H), 126.4 (s, IrNNCHC***C***H), 125.7 (s, IrNCH***C***), 124.0 (IrCN***C***H), 97.3 (s, Ir***C***H), 95.3 (s, Ir***C***H), 83.1 (s, Ir***C***H), 78.6 (s, Ir***C***H), 19.8 (s,

NCC(CH_3)CHC(***C***H_3)), 17.6 (s, NCC(***C***H_3)), 16.5 (s, NCC(CH_3)). ^{15}N NMR (methanol-d_4, 500 MHz): 368.9 (IrN***N***), 266.6 (Ir***N***N), 198.0 (IrC***N***).

[Ir(H)$_2$(IMes)(pdz)$_3$]Cl (4a) and [Ir(H)$_2$(IMes)(phth)$_3$]Cl (4c)

The numbering scheme used for the NMR assignments is presented in sScheme 1:

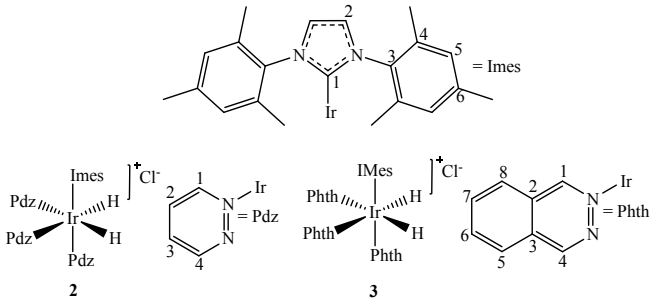

sScheme 1: Active complexes 4a and 4b formed with pyridazine and phthalazine respectively. The numbering scheme for NMR assignment is indicated.

NMR observations with [Ir(H)$_2$(IMes)(pdz)$_3$]Cl (**4a**).

1 (2 mg, 3.12 µmol) and five equivalents of pyridazine (1.13 µL, 15.6 µmol) were dissolved in Methanol-d4 (0.5 mL) in a 5 mm NMR tube and degassed. H_2 (3 bar) was added and the sample was heated to 348 K for 15 minutes to fully activate the complex and form **4a** in solution. Characterisation data is presented below. ^{1}H NMR (500 MHz, methanol-d$_4$, 298 K): δ 9.62 (d.d, *J* = 5.6, 2.4 Hz, 1H, ax. pdz. 1), 9.32 (d.d, *J* = 5.6, 2.4 Hz, 2H, eq. pdz. 1), 8.76 (d.d, *J* = 4.8, 3.0 Hz, 2H, eq. pdz. 4), 8.29 (d.d, *J* = 4.8, 3.0 Hz, 1H, ax. pdz. 4), 7.62 (m, 2H, eq. pdz. 2), 7.48 (m, 1H, ax. pdz. 2), 7.42 (m, 1H, ax. pdz. 3), 7.39 (m, 2H, eq. pdz. 3), 7.09 (s, 2H, IMes 2), 6.69 (s, 4H, IMes 5), 2.22 (s, 6H, IMes C*H$_3$*), 2.04 (s, 12H, IMes C*H$_3$*), -21.47 (s, 2H, Ir*H*). ^{13}C NMR (125 MHz, methanol-d$_4$, 298 K): δ 162.0 (s, ax. pdz. 1), 157.8 (s, eq. pdz. 1), 152.4 (s, ax. pdz. 4), 151.5 (s, eq. pdz. 4), 129.6 (s, ax. pdz. 3), 129.2 (s, eq. pdz. 3), 126.3 (s, ax. pdz. 2), 126.1 (s, eq. pdz. 2), 151.7, (s, IMes 1), 138.1 (s, IMes 6), 137.5 (s, IMes 4), 135.4 (s, IMes 3), 128.4 (s, IMes 5), 122.4 (s, IMes 2), 19.5 (s, IMes *C*H$_3$), 17.3 (s, IMes *C*H$_3$). ^{15}N NMR (50.7 MHz, methanol-d4, 253 K): δ 392.2 (s, ax. pdz. IrN*N*), 390.0 (s, eq. pdz. IrN*N*), 326.2 (s, eq. pdz. Ir*N*), 305.8 (s, ax. pdz. Ir*N*), 194.5 (s, IMes), free pyridazine = 349.3.

Preparation of [Ir(H)$_2$(IMes)(phth)$_3$]Cl (**4b**).

1 (2 mg, 3.12 µmol) and five equivalents of phthalazine (2.03 mg, 15.6 µmol) were dissolved in methanol-d$_4$ (0.5 mL) in a 5 mm NMR tube and degassed. H_2 (3 bar) was added and the sample was heated to 348 K for 15 minutes to fully activate the complex and form **4b** in solution. ^{1}H NMR (500 MHz, methanol-d$_4$, 298 K): δ 10.28 (s, 1H, ax. phth. 1), 10.16 (s, 2H, eq. phth. 1), 9.27 (s, 2H, eq. phth. 4), 8.60 (s, 1H, ax. phth. 4), 8.18 (m, 2H, eq. phth. 5), 8.17 (m, 1H, ax. phth. 8), 8.12 (m, 2H, eq. phth. 7), 8.09 (m, 2H, eq. phth. 6), 8.07 (m, 1H, ax. phth. 7), 8.00 (m, 2H, eq. phth. 8), 7.99 (m, 1H, ax. phth. 6), 7.78 (m, 1H, ax. phth. 5), 7.15 (s, 2H, IMes 2), 6.37 (s, 4H, IMes 5), 2.07 (s, 12H, IMes C*H$_3$*), 1.92 (s, 6H, IMes C*H$_3$*), -21.00 (s, 2H, Ir*H*). ^{13}C NMR (125 MHz, methanol-d$_4$, 298 K): δ 160.9 (s, ax. phth. 1), 157.0 (s, eq. phth. 1), 151.9 (s, ax. phth. 4), 151.0 (s, eq. phth. 4), 133.6 (s, ax. phth. 6), 133.6 (s, eq. phth. 7), 133.3 (s, ax. phth. 7), 133.3 (s, eq. phth. 6), 128.3 (s, ax. phth. 2), 128.1 (s, eq. phth. 2), 126.6 (s, eq. phth. 8), 126.3 (s, ax. phth. 8), 126.3 (s, eq. phth. 5), 126.2 (s, ax. phth. 5), 125.5 (s, eq. phth. 3), 125.0 (s, ax. phth. 3), 151.8 (s, IMes 1), 137.9 (s, IMes 6), 137.3 (s, IMes 4), 135.2 (s, IMes 3), 128.2 (s, IMes 5), 122.4 (s, IMes 2), 19.6 (s, IMes *C*H$_3$), 17.5 (s, IMes *C*H$_3$). ^{15}N NMR (50.7 MHz, methanol-d4, 253 K): δ 362.8 (s, ax. phth. IrN*N*), 360.9 (s, eq. phth. IrN*N*), 299.7 (s, eq. phth. Ir*N*), 278.8 (s, ax. phth. Ir*N*), 194.3 (s, IMes), free phthalazine = 349.6.

The imbalance that is observed in the hydride ligand signal intensities that are seen in these NMR spectra is a consequence of two effects, the different line widths of the resonances and the detection of signals that are derived from $I_z^1 I_z^2$, $-I_z^1$ and $+I_z^2$ terms, with relative proportions of 1 : 0.0625 : 0.0625. These three product operators reflect the magnetic states that are created as a result of PHIP.[24]

2. Hydride and substrate ligand exchange dynamics

sTable 1: Change in chemical shift of free pyridazine and phthalazine on binding to iridium to form 2a and 2b.

	2a	**Δδ**	**2b**	**Δδ**
^{15}N Ir-**N**=N-	386.1	-58.2	386.0	-36.7
^{15}N Ir-N=**N**-	311.8	16.1	311.5	37.8

sTable 2: Rate constants for haptotropic shifts, detected via selective 1D-EXSY methods at the specified temperatures.

Temperature / K	Rate of Haptotropic shift / s^{-1}	
	2a	**2b**
235	-	0.923 ± 0.001
240	0.729 ± 0.001	1.873 ± 0.003
245	1.501 ± 0.003	3.955 ± 0.003
250	3.155 ± 0.002	7.318 ± 0.004
255	5.80 ± 0.01	13.426 ± 0.004
260	12.74 ± 0.02	-

sTable 3: Experimentally determined activation parameters for haptotropic shifts in 2a and 2b in methanol-d_4.

Complex	**$\Delta H^{\ddagger}$ / kJ mol^{-1}**	**$\Delta S^{\ddagger}$ / J mol^{-1} K^{-1}**	**$\Delta G^{\ddagger}$ / kJ mol^{-1} (300 K)**
2a	71.3 ± 0.3	57 ± 1	54.2 ± 0.4
2b	66.0 ± 0.1	43.0 ± 0.6	53.1 ± 0.2

sTable 4: Rate constants for ligand exchange detected via selective 1D-EXSY methods at the specified temperatures.

Temp. /K	Rate of substrate dissociation/s^{-1}		Rate of H_2 dissociation/s^{-1}		Rate of substrate haptotropic shift/s^{-1}	
	4a	**4b**	**4a**	**4b**	**4a**	**4b**
280	0.0454 ± 0.0002	0.0603 ± 0.0003	0.091 ± 0.005	0.094 ± 0.005	0.0376 ± 0.0001	0.0326 ± 0.0002
285	0.0986 ± 0.0001	0.1153 ± 0.0003	0.183 ± 0.003	0.169 ± 0.005	0.0942 ± 0.0002	0.0697 ± 0.0004
290	0.1926 ± 0.0002	0.2110 ± 0.0003	0.347 ± 0.008	0.33 ± 0.01	0.1925 ± 0.0003	0.1419 ± 0.0005
295	0.3611 ± 0.0008	0.382 ± 0.001	0.70 ± 0.02	0.59 ± 0.08	0.4078 ± 0.0008	0.3212 ± 0.0008
300/301	0.642 ± 0.003	0.663 ± 0.003	1.46 ± 0.01	1.12 ± 0.03	0.819 ± 0.02	0.673 ± 0.002
305	1.073 ± 0.006	1.085 ± 0.005	2.83 ± 0.06	1.69 ± 0.05	1.203 ± 0.005	1.103 ± 0.003
310	1.61 ± 0.02	1.69 ± 0.02	5.1 ± 0.1	3.11 ± 0.08	1.84 ± 0.04	1.98 ± 0.01
315	4.81 ± 0.01	3.03 ± 0.02	-	5.4 ± 0.1	5.01 ± 0.03	3.43 ± 0.02
320	8.93 ± 0.03	4.69 ± 0.03	-	9.3 ± 0.1	9.36 ± 0.04	5.69 ± 0.03
325	-	7.57 ± 0.03	-	16.0 ± 0.5	-	8.22 ± 0.05

sTable 5: Experimentally-determined activation parameters for indicated ligand exchange processes in 4a and 4b in Methanol-d4

Process	$\Delta H^{\ddagger}$ /kJ mol^{-1}		$\Delta S^{\ddagger}$ / J K^{-1} mol^{-1}		$\Delta G^{\ddagger}_{(300\ K)}$ /kJ mol^{-1}	
Complex	**2c**	**3c**	**2c**	**3c**	**2c**	**3c**
Substrate Haptotropic Shift	97.9 ± 0.3	92.0 ± 0.3	85 ± 1	62 ± 1	72.5 ± 0.3	73.3 ± 0.3
Substrate Dissociation	94.3 ± 0.4	78.13 ± 0.06	72 ± 1	17.4 ± 0.2	72.6 ± 0.3	72.93 ± 0.06
H_2 loss	95.6 ± 0.2	83.6 ± 0.1	82.4 ± 0.8	39.8 ± 0.4	70.9 ± 0.3	71.6 ± 0.2

sTable 6: Ligand exchange rate constants for 4a as a function of [pdz].

[free pdz]/mM	Rate of pdz dissociation/s^{-1}	Rate of pdz haptotropic shift / s^{-1}	Rate of H_2 dissociation/s^{-1}
17.35	0.0986 ± 0.0001	0.0942 ± 0.0001	0.183 ± 0.003
27.64	0.0982 ± 0.0002	0.0914 ± 0.0002	0.120 ± 0.003
63.27	0.0994 ± 0.0002	0.0955 ± 0.0002	0.052 ± 0.001
85.55	0.1017 ± 0.0003	0.0945 ± 0.0002	0.037 ± 0.001
115.75	0.0989 ± 0.0002	0.0932 ± 0.0003	0.029 ± 0.001

sTable 7: Ligand exchange rate constants for 2b as a function of [phth].

[free phth]/mM	Rate of phth dissociation/s^{-1}	Rate of phth haptotropic shift / s^{-1}	Rate of H_2 dissociation/s^{-1}
6.99	0.1001 ± 0.0001	0.0618 ± 0.0001	0.243 ± 0.007
19.22	0.1192 ± 0.0002	0.0711 ± 0.0002	0.172 ± 0.004
40.44	0.1168 ± 0.0003	0.0694 ± 0.0003	0.119 ± 0.005
78.56	0.1037 ± 0.0002	0.0630 ± 0.0001	0.083 ± 0.005
121.80	0.1000 ± 0.0002	0.0615 ± 0.0001	0.0643 ± 0.003

sTable 8: Ligand exchange rate constants for 4a as a function of [H_2].

H_2 pressure / bar	Rate of pdz dissociation / s^{-1}	Rate of pdz haptotropic shift / s^{-1}	Rate of H_2 dissociation / s^{-1}
0.445	**0.466 ± 0.003**	**0.800 ± 0.001**	**0.428 ± 0.001**
1.032	**0.456 ± 0.003**	**0.797 ± 0.001**	**0.790 ± 0.003**
1.515	**0.456 ± 0.003**	**0.780 ± 0.001**	**0.94 ± 0.02**
2.000	**0.451 ± 0.003**	**0.778 ± 0.002**	**1.03 ± 0.01**
2.495	**0.456 ± 0.003**	**0.785 ± 0.002**	**1.10 ± 0.02**
2.990	**0.458 ± 0.003**	**0.780 ± 0.001**	**1.16 ± 0.03**

3. Mechanism of H_2 loss

sTable 9: H_2 exchange rate constants for 4a as a function of [pdz].

[free pdz]/mM	Rate of H_2 dissociation/s^{-1}	1/Rate of H_2 dissociation/s
17.35	0.183 ± 0.003	5.46 ± 0.09
27.64	0.120 ± 0.003	8.3 ± 0.2
63.27	0.052 ± 0.001	19.2 ± 0.4
85.55	0.037 ± 0.001	26.8 ± 0.7
115.75	0.029 ± 0.001	34 ± 1

sTable 10: H_2 exchange rate constants for 2b as a function of [phth].

[free phth]/mM	Rate of H_2 dissociation/s^{-1}	1/Rate of H_2 dissociation/s
6.99	0.243 ± 0.007	4.1 ± 0.1
19.22	0.172 ± 0.004	5.8 ± 0.1
40.44	0.119 ± 0.005	8.4 ± 0.4
78.56	0.083 ± 0.005	12.1 ± 0.7
121.80	0.0643 ± 0.003	15.6 ± 0.7

4. SABRE enhancements achieved using 4a and 4b vary with [substrate]

sTable 11: Enhancements in free pdz using 4a, as a function of [pdz].

[free pdz]/mM	Enhancement Factor			
	NC***H***	NCHC***H***	Total	1/Total
17.35	-379 ± 1	-37 ± 1	-832 ± 3	-0.001202 ± 0.000004
27.64	-112 ± 1	-15 ± 1	-254 ± 3	-0.00394 ± 0.00005
63.27	-35 ± 1	-8 ± 1	-85 ± 3	-0.0118 ± 0.0004
85.55	-21 ± 1	-5 ± 1	-53 ± 3	-0.019 ± 0.001
115.75	-12 ± 1	-3 ± 1	-29 ± 3	-0.034 ± 0.004

sTable 12: Enhancements in free phth using 4b, as a function of [phth].

[free phth]/mM	Enhancement Factor				
	NC***H***	NCHCC***H***	NCHCCHC***H***	Total	1/Total
37.56	-65 ± 1	-13 ± 1	-3 ± 1	-164 ± 3	-0.0061 ± 0.0001
59.84	-32 ± 1	-7 ± 1	-3 ± 1	-85 ± 3	-0.0118 ± 0.0004
78.56	-25 ± 1	-4 ± 1	-1 ± 1	-60 ± 3	-0.0167 ± 0.0008
104.08	-18 ± 1	-2 ± 1	0 ± 1	-39 ± 3	-0.025 ± 0.002
121.80	-12 ± 1	-1 ± 1	0 ± 1	-27 ± 3	-0.037 ± 0.004

5. SABRE enhancements achieved using 4a and 4b vary with temperature

sTable 13: Enhancements in free pdz using 4a, as a function of temperature.

Temperature / K	Enhancement Factor		
	NC***H***	NCHC***H***	Total
273.2	-54 ± 1	-4 ± 1	-116 ± 3
293.2	-105 ± 1	-11 ± 1	-233 ± 3
303.2	-132 ± 1	-16 ± 1	-297 ± 3
313.2	-165 ± 1	-29 ± 1	-387 ± 3
323.2	-186 ± 1	-33 ± 1	-438 ± 3

sTable 14: Enhancements in free phth using 4b, as a function of temperature.

Temperature / K	Enhancement Factor			
	NC***H***	NCHCC***H***	NCHCCHC***H***	Total
273.2	-84 ± 1	-10 ± 1	-4 ±1	-195 ± 3
293.2	-161 ± 1	-18 ± 1	-9 ± 1	-376 ± 3
303.2	-207 ± 1	-31 ± 1	-13 ± 1	-501 ± 3
313.2	-257 ± 1	-38 ± 1	-16 ± 1	-622 ± 3
323.2	-292 ± 1	-42 ± 1	-19 ± 1	-708 ± 3

6. SABRE enhancements using 4a vary with dilution

sTable 15: Enhancements in free pdz using 4a, as a function of dilution, with 4.07 equivalents of free pyridazine in solution.

[2]/mM	Enhancement Factor			Signal to noise ratio		
	NC***H***	NCHC***H***	Total	NC***H***	NCHC***H***	Total
6.24	-232 ± 1	-24 ± 1	-511 ± 3	18840	3400	22240
4.16	-476 ± 1	-46 ± 1	-1044 ± 3	16800	3130	19930
2.77	-568 ± 1	-71 ± 1	-1278 ± 3	18400	5500	23910
1.23	-573 ± 1	-67 ± 1	-1280 ± 3	9120	1760	10880

7. SABRE enhancements using 4a and 4b vary with PTF: detection of longitudinal magnetisation

SABRE creates higher order magnetic terms which are optimally enhanced at different field values.[70] For pyridazine, these are exemplified by four two spin order combinations ($2I_zI_z$, $2S_zS_z$, $2I_zS_z$, $2I_zS'_z$), two three spin order combinations (*eg* $4I_zS_zS'_z$) and one four spin order term ($8I_zS_zI'_zS'_z$). These states were quantified using the only parahydrogen spectroscopy (OPSY) protocol.[71, 72] The single spin terms proved to be created more efficiently than two spin terms which in turn exceed those of three and four spin combinations.

Pyridazine NC***H*** resonance

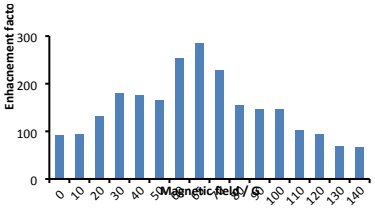

sFigure 1: PTF plot, normalized for the state selection process, over the range 0 to 140 G, for the NC*H* resonance in free pdz using 4a.

sTable 16: Enhancements in the NC*H* resonance of free pdz using 4a, as a function of PTF.

Field / G	Enhancement Factor		Correction for Receiver Gain (/1)
	NC***H***	Total	
0	46 ± 1	92 ± 2	92 ± 2
10	47 ± 1	93 ± 2	93 ± 2
20	66 ± 1	132 ± 2	132 ± 2
30	90 ± 1	179 ± 2	179 ± 2
40	88 ± 1	176 ± 2	176 ± 2
50	83 ± 1	165 ± 2	165 ± 2
60	126 ± 1	253 ± 2	253 ± 2
65	142 ± 1	284 ± 2	284 ± 2
70	114 ± 1	228 ± 2	228 ± 2
80	77 ± 1	154 ± 2	154 ± 2
90	73 ± 1	146 ± 2	146 ± 2
100	73 ± 1	146 ± 2	146 ± 2
110	51 ± 1	102 ± 2	102 ± 2
120	46 ± 1	93 ± 2	93 ± 2
130	34 ± 1	68 ± 2	68 ± 2
140	33 ± 1	66 ± 2	66 ± 2

Pyridazine NCHC***H*** resonance

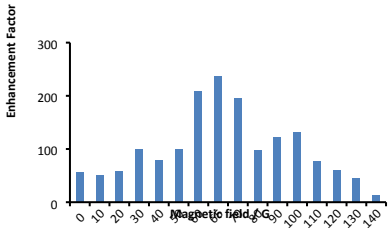

sFigure 2: PTF plot, normalized for the state selection process, over the range 0 to 140 G, for the NCHC*H* resonance of free pdz using 4a.

sTable 17: Enhancements in the NCHC*H* resonance of free pdz using 4a, as a function of PTF.

Field / G	Enhancement Factor		Correction for Receiver Gain (/1)
	NCHC***H***	Total	
0	28 ± 1	56 ± 2	56 ± 2
10	25 ± 1	50 ± 2	50 ± 2
20	30 ± 1	59 ± 2	59 ± 2
30	50 ± 1	100 ± 2	100 ± 2
40	40 ± 1	79 ± 2	79 ± 2
50	50 ± 1	100 ± 2	100 ± 2
60	105 ± 1	209 ± 2	209 ± 2
65	119 ± 1	238 ± 2	238 ± 2
70	98 ± 1	195 ± 2	195 ± 2
80	49 ± 1	98 ± 2	98 ± 2
90	61 ± 1	122 ± 2	122 ± 2
100	66 ± 1	132 ± 2	132 ± 2
110	39 ± 1	77 ± 2	77 ± 2
120	30 ± 1	60 ± 2	60 ± 2
130	23 ± 1	45 ± 2	45 ± 2
140	6 ± 1	12 ± 2	12 ± 2

Pyridazine single quantum coherences

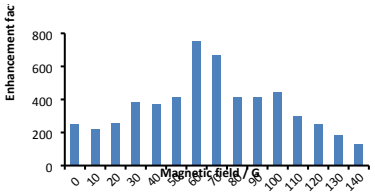

sFigure 3: PTF plot, normalized for the state selection process, over the range 0 to 140 G, for the single quantum coherences in free phth using 4b.

sTable 18: Enhancements in the single quantum coherence resonances of free pthh using 4b, as a function of PTF.

Field / G	Enhancement Factor			Correction for observation of 1 of 2 terms	Correction for Receiver Gain (/1)
	NC***H***	NCHC***H***	Total		
0	45 ± 2	18 ± 2	127 ± 6	250 ± 10	250 ± 10
10	42 ± 2	12 ± 2	110 ± 6	220 ± 10	220 ± 10
20	59 ± 2	4 ± 2	127 ± 6	250 ± 10	250 ± 10
30	79 ± 2	17 ± 2	192 ± 6	380 ± 10	380 ± 10
40	78 ± 2	15 ± 2	185 ± 6	370 ± 10	370 ± 10
50	75 ± 2	29 ± 2	208 ± 6	420 ± 10	420 ± 10
60	114 ± 2	75 ± 2	377 ± 6	750 ± 10	750 ± 10
70	102 ± 2	66 ± 2	336 ± 6	670 ± 10	670 ± 10
80	68 ± 2	36 ± 2	208 ± 6	420 ± 10	420 ± 10
90	59 ± 2	45 ± 2	208 ± 6	420 ± 10	420 ± 10
100	62 ± 2	49 ± 2	222 ± 6	440 ± 10	440 ± 10
110	47 ± 2	28 ± 2	148 ± 6	300 ± 10	300 ± 10
120	40 ± 2	23 ± 2	126 ± 6	250 ± 10	250 ± 10
130	30 ± 2	16 ± 2	92 ± 6	180 ± 10	180 ± 10
140	31 ± 2	3 ± 2	66 ± 6	130 ± 10	130 ± 10

Phthalazine NC***H***

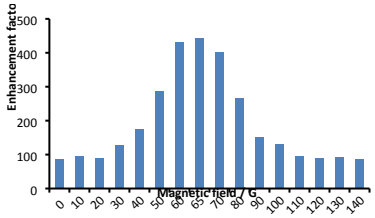

sFigure 4: PTF plot, normalized for the state selection process, over the range 0 to 140 G, for the NC*H* resonance in free phth using 4b.

sTable 19: Enhancements in the NC*H* resonance of free phth using 4b, as a function of PTF.

Field / G	Enhancement Factor		Correction for Receiver Gain (/1)
	NC***H***	Total	
0	43 ± 2	86 ± 4	86 ± 4
10	48 ± 2	96 ± 4	96 ± 4
20	45 ± 2	90 ± 4	90 ± 4
30	64 ± 2	129 ± 4	129 ± 4
40	88 ± 2	176 ± 4	176 ± 4
50	143 ± 2	287 ± 4	287 ± 4
60	217 ± 2	433 ± 4	433 ± 4
65	222 ± 2	443 ± 4	443 ± 4
70	201 ± 2	402 ± 4	402 ± 4
80	133 ± 2	266 ± 4	266 ± 4
90	76 ± 2	153 ± 4	153 ± 4
100	65 ± 2	131 ± 4	131 ± 4
110	48 ± 2	96 ± 4	96 ± 4
120	45 ± 2	90 ± 4	90 ± 4
130	46 ± 2	93 ± 4	93 ± 4
140	44 ± 2	88 ± 4	88 ± 4

Phthalazine NCHCC***H***

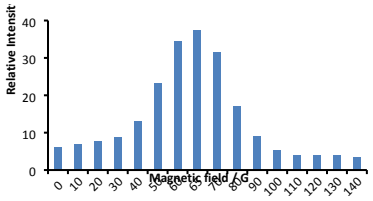

sFigure 5: PTF plot, normalized for the state selection process, over the range 0 to 140 G, for the NCHCC*H* resonance of free phth using 4b.

sTable 20: Enhancements in the NCHCC*H* resonance of free phth using 4b, as a function of PTF.

Field / G	Enhancement Factor		Correction for Receiver Gain (/1)
	NCHCC*H*	Total	
0	3.0 ± 0.1	5.9 ± 0.2	5.9 ± 0.2
10	3.4 ± 0.1	6.8 ± 0.2	6.8 ± 0.2
20	3.8 ± 0.1	7.5 ± 0.2	7.5 ± 0.2
30	4.4 ± 0.1	8.8 ± 0.2	8.8 ± 0.2
40	6.5 ± 0.1	13.0 ± 0.2	13.0 ± 0.2
50	11.7 ± 0.1	23.3 ± 0.2	23.3 ± 0.2
60	17.2 ± 0.1	34.5 ± 0.2	34.5 ± 0.2
65	18.7 ± 0.1	37.4 ± 0.2	37.4 ± 0.2
70	15.7 ± 0.1	31.5 ± 0.2	31.5 ± 0.2
80	8.5 ± 0.1	17.0 ± 0.2	17.0 ± 0.2
90	4.4 ± 0.1	8.9 ± 0.2	8.9 ± 0.2
100	2.7 ± 0.1	5.4 ± 0.2	5.4 ± 0.2
110	2.0 ± 0.1	4.0 ± 0.2	4.0 ± 0.2
120	1.9 ± 0.1	3.8 ± 0.2	3.8 ± 0.2
130	2.0 ± 0.1	4.0 ± 0.2	4.0 ± 0.2
140	1.6 ± 0.1	3.3 ± 0.2	3.3 ± 0.2

Phthalazine NCHCCHC***H***

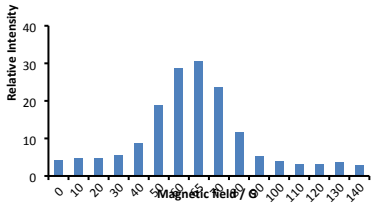

sFigure 6: PTF plot, normalized for the state selection process, over the range 0 to 140 G, for the NCHCCHC*H* resonance in free phth using 4b.

sTable 21: Enhancements in the NCHCCHC*H* resonance of free phth using 4b, as a function of PTF.

Field / G	Enhancement Factor		Correction for Receiver Gain (/1)
	NCHCCHC*H*	Total	
0	2.1 ± 0.1	4.2 ± 0.2	4.2 ± 0.2
10	2.3 ± 0.1	4.6 ± 0.2	4.6 ± 0.2
20	2.3 ± 0.1	4.6 ± 0.2	4.6 ± 0.2
30	2.7 ± 0.1	5.5 ± 0.2	5.5 ± 0.2
40	4.3 ± 0.1	8.6 ± 0.2	8.6 ± 0.2
50	9.4 ± 0.1	18.8 ± 0.2	18.8 ± 0.2
60	14.3 ± 0.1	28.5 ± 0.2	28.5 ± 0.2
65	15.3 ± 0.1	30.5 ± 0.2	30.5 ± 0.2
70	11.8 ± 0.1	23.5 ± 0.2	23.5 ± 0.2
80	5.7 ± 0.1	11.5 ± 0.2	11.5 ± 0.2
90	2.6 ± 0.1	5.2 ± 0.2	5.2 ± 0.2
100	1.9 ± 0.1	3.9 ± 0.2	3.9 ± 0.2
110	1.5 ± 0.1	3.0 ± 0.2	3.0 ± 0.2
120	1.6 ± 0.1	3.1 ± 0.2	3.1 ± 0.2
130	1.8 ± 0.1	3.5 ± 0.2	3.5 ± 0.2

140	1.4 ± 0.1	2.8 ± 0.2	2.8 ± 0.2

Phthalazine single quantum terms

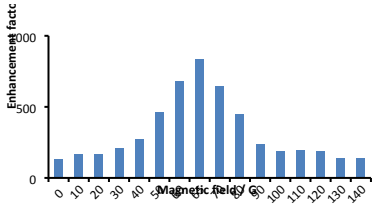

sFigure 7: PTF plot, normalized for the state selection process, over the range 0 to 140 G, for the single quantum coherence resonances in free phth using 4b.

sTable 22: Enhancements in the single quantum coherence resonances of free phth using 4b, as a function of PTF.

Field / G	Enhancement Factor					
	NC***H***	NCHCC***H***	NCHCCHC***H***	Total	Correction for observation of 1 of 2 terms	Correction for Receiver Gain (/1)
0	29.0 ± 0.6	2.9 ± 0.2	0.8 ± 0.1	65 ± 1	130 ± 2	130 ± 2
10	37.2 ± 0.6	4.0 ± 0.2	0.9 ± 0.1	84 ± 1	168 ± 2	168 ± 2
20	36.7 ± 0.6	4.3 ± 0.2	0.8 ± 0.1	84 ± 1	167 ± 2	167 ± 2
30	45.1 ± 0.6	5.7 ± 0.2	1.8 ± 0.1	105 ± 1	211 ± 2	211 ± 2
40	55.6 ± 0.6	8.2 ± 0.2	4.4 ± 0.1	136 ± 1	273 ± 2	273 ± 2
50	90.0 ± 0.6	14.9 ± 0.2	11.2 ± 0.1	232 ± 1	464 ± 2	464 ± 2
60	130.8 ± 0.6	22.0 ± 0.2	17.1 ± 0.1	340 ± 1	679 ± 2	679 ± 2
65	161.4 ± 0.6	27.0 ± 0.2	20.0 ± 0.1	417 ± 1	833 ± 2	833 ± 2
70	126.1 ± 0.6	20.0 ± 0.2	14.0 ± 0.1	320 ± 1	640 ± 2	640 ± 2
80	92.0 ± 0.6	12.0 ± 0.2	7.4 ± 0.1	223 ± 1	446 ± 2	446 ± 2
90	50.1 ± 0.6	5.3 ± 0.2	3.0 ± 0.1	117 ± 1	234 ± 2	234 ± 2
100	40.5 ± 0.6	3.5 ± 0.2	2.2 ± 0.1	93 ± 1	185 ± 2	185 ± 2
110	43.7 ± 0.6	3.0 ± 0.2	1.9 ± 0.1	97 ± 1	194 ± 2	194 ± 2
120	42.7 ± 0.6	2.6 ± 0.2	1.4 ± 0.1	93 ± 1	187 ± 2	187 ± 2
130	32.1 ± 0.6	2.0 ± 0.2	0.5 ± 0.1	69 ± 1	139 ± 2	139 ± 2
140	31.3 ± 0.6	1.9 ± 0.2	0.4 ± 0.1	67 ± 1	134 ± 2	134 ± 2

8. SABRE enhancements using 4a and 4b vary with PTF: detection of longitudinal two-spin and higher order terms

Pyridazine NCHC***H*** double quantum state

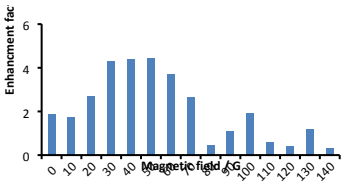

sFigure 8: PTF plot, normalized for the state selection process, over the range 0 to 140 G, for the S_ZS_Z term associated with the two chemically equivalent NCHC*H* in free pdz using 4a.

sTable 23: Enhancements in the NCHC*H* double quantum resonances of free pdz using 4a, as a function of PTF.

Field / G	Enhancement Factor		Correction for observation of 1 of 4 terms	Correction for Receiver Gain (/16)
	NCHC***H***	Total		
0	3.7 ± 0.2	7.4 ± 0.4	30 ± 2	1.9 ± 0.1
10	3.5 ± 0.2	7.0 ± 0.4	28 ± 2	1.8 ± 0.1
20	5.3 ± 0.2	10.7 ± 0.4	43 ± 2	2.7 ± 0.1
30	8.6 ± 0.2	17.1 ± 0.4	68 ± 2	4.3 ± 0.1
40	8.8 ± 0.2	17.6 ± 0.4	70 ± 2	4.4 ± 0.1
50	8.9 ± 0.2	17.8 ± 0.4	71 ± 2	4.5 ± 0.1
60	7.4 ± 0.2	14.8 ± 0.4	59 ± 2	3.7 ± 0.1
70	5.3 ± 0.2	10.6 ± 0.4	42 ± 2	2.7 ± 0.1
80	0.9 ± 0.2	1.8 ± 0.4	7 ± 2	0.5 ± 0.1
90	2.2 ± 0.2	4.4 ± 0.4	18 ± 2	1.1 ± 0.1
100	3.8 ± 0.2	7.6 ± 0.4	30 ± 2	1.9 ± 0.1
110	1.2 ± 0.2	2.3 ± 0.4	9 ± 2	0.58 ± 0.1
120	0.8 ± 0.2	1.6 ± 0.4	6 ± 2	0.4 ± 0.1
130	2.4 ± 0.2	4.7 ± 0.4	19 ± 2	1.18 ± 0.1
140	0.6 ± 0.2	1.2 ± 0.4	5 ± 2	0.3 ± 0.1

Pyridazine double quantum

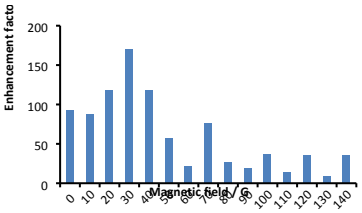

sFigure 9: PTF plot, normalized for the state selection process, over the range 0 to 140 G, for the double quantum coherence resonances in free pdz using 4a.

sTable 24: Enhancements in the double quantum resonances of free pdz using 4a, as a function of PTF.

Field / G	Enhancement Factor				
	NC***H***	NCHC***H***	Total	Correction for observation of 1 of 4 terms	Correction for Receiver Gain (/16)
0	87 ± 7	97 ± 8	370 ± 20	1480 ± 80	92 ±5
10	83 ± 7	93 ± 8	350 ± 20	1410 ± 80	88 ±5
20	111 ± 7	126 ± 8	470 ± 20	1900 ± 80	119 ±5
30	159 ± 7	182 ± 8	680 ± 20	2730 ± 80	170 ±5
40	109 ± 7	126 ± 8	470 ± 20	1880 ± 80	118 ±5
50	52 ± 7	63 ± 8	230 ± 20	920 ± 80	57 ±5
60	19 ± 7	24 ± 8	90 ± 20	350 ± 80	22 ±5
70	71 ± 7	82 ± 8	310 ± 20	1220 ± 80	76 ±5
80	26 ± 7	27 ± 8	100 ± 20	420 ± 80	26 ±5
90	19 ± 7	20 ± 8	80 ± 20	310 ± 80	20 ±5
100	33 ± 7	40 ± 8	150 ± 20	590 ± 80	37 ±5
110	13 ± 7	14 ± 8	50 ± 20	220 ± 80	14 ±5
120	32 ± 7	38 ± 8	150 ± 20	560 ± 80	35 ±5
130	9 ± 7	7 ± 8	30 ± 20	130 ± 80	8 ±5
140	33 ± 7	37 ± 8	140 ± 20	560 ± 80	35 ±5

Pyridazine triple quantum

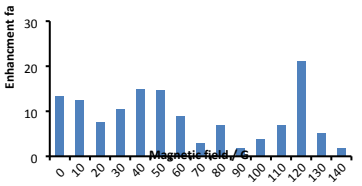

sFigure 10: PTF plot, normalized for the state selection process, over the range 0 to 140 G, for the triple quantum coherence resonances in free pdz using 4a.

sTable 25: Enhancements in the triple quantum resonances of pdz using 4a, as a function of PTF.

Field / G	Enhancement Factor				
	NC***H***	NCHC***H***	Total	Correction for observation of 1 of 8 terms	Correction for Receiver Gain (/912)
0	500 ± 70	270 ± 70	1500 ± 200	6100 ± 800	13 ± 2
10	420 ± 70	290 ± 70	1400 ± 200	5700 ± 800	13 ± 2
20	330 ± 70	100 ± 70	900 ± 200	3400 ± 800	8 ± 2
30	340 ± 70	250 ± 70	1200 ± 200	4700 ± 800	10 ± 2
40	120 ± 70	730 ± 70	1700 ± 200	6800 ± 800	15 ± 2
50	200 ± 70	640 ± 70	1700 ± 200	6700 ± 800	15 ± 2
60	90 ± 70	410 ± 70	1000 ± 200	4000 ± 800	9 ± 2
70	50 ± 70	130 ± 70	300 ± 200	1400 ± 800	3 ± 2
80	240 ± 70	160 ± 70	800 ± 200	3200 ± 800	7 ± 2
90	20 ± 70	90 ± 70	200 ± 200	900 ± 800	2 ± 2
100	170 ± 70	40 ± 70	400 ± 200	1700 ± 800	4 ± 2
110	110 ± 70	280 ± 70	800 ± 200	3100 ± 800	7 ± 2
120	710 ± 70	490 ± 70	2400 ± 200	9600 ± 800	21 ± 2
130	170 ± 70	120 ± 70	600 ± 200	2300 ± 800	5 ± 2
140	40 ± 70	60 ± 70	200 ± 200	800 ± 800	2 ± 2

Pyridazine quadruple quantum

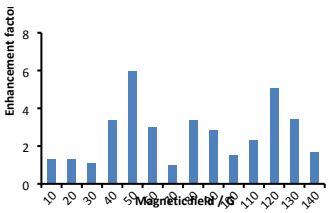

sFigure 11: PTF plot, normalized for the state selection process, over the range 0 to 140 G, for the quadruple quantum coherence resonances in free pdz using 4a.

sTable 26: Enhancements in the quadruple quantum resonances of free pdz using 4a, as a function of PTF.

Field / G	Enhancement Factor				
	NC***H***	NCHC***H***	Total	Correction for observation of 1 of 16 terms	Correction for Receiver Gain (/2050)
0	-	-	-	-	-
10	35 ± 2	50 ± 4	169 ± 9	2700 ± 100	1.32 ± 0.05
20	35 ± 2	48 ± 4	165 ± 9	2600 ± 100	1.29 ± 0.05
30	29 ± 2	42 ± 4	141 ± 9	2300 ± 100	1.10 ± 0.05
40	85 ± 2	129 ± 4	428 ± 9	6800 ± 100	3.34 ± 0.05
50	155 ± 2	230 ± 4	764 ± 9	12200 ± 100	5.97 ± 0.05
60	76 ± 2	114 ± 4	381 ± 9	6100 ± 100	2.97 ± 0.05
70	27 ± 2	35 ± 4	123 ± 9	2000 ± 100	0.96 ± 0.05
80	88 ± 2	126 ± 4	428 ± 9	6800 ± 100	3.34 ± 0.05
90	71 ± 2	110 ± 4	363 ± 9	5800 ± 100	2.83 ± 0.05
100	39 ± 2	56 ± 4	190 ± 9	3000 ± 100	1.48 ± 0.05
110	60 ± 2	89 ± 4	297 ± 9	4800 ± 100	2.32 ± 0.05
120	133 ± 2	192 ± 4	648 ± 9	10400 ± 100	5.06 ± 0.05
130	88 ± 2	132 ± 4	439 ± 9	7000 ± 100	3.43 ± 0.05
140	44 ± 2	63 ± 4	214 ± 9	3400 ± 100	1.67 ± 0.05

Phthalazine double quantum terms

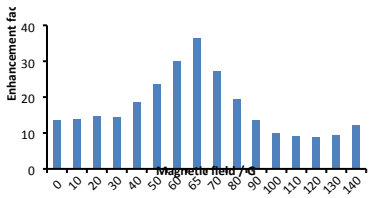

sFigure 12: PTF plot, normalized for the state selection process, over the range 0 to 140 G, for the double quantum coherence resonances in free phth, using 4b.

sTable 27: Enhancements in the double quantum coherence resonances of free phth using 4b, as a function of PTF.

Field / G	Enhancement Factor					
	NC***H***	NCHCC***H***	NCHCCHC***H***	Total	Correction for observation of 1 of 4 terms	Correction for Receiver Gain (/128)
0	13 ± 1	105 ± 8	99 ± 8	440 ± 30	1700 ± 100	13.6 ± 0.8
10	16 ± 1	105 ± 8	99 ± 8	440 ± 30	1800 ± 100	13.8 ± 0.8
20	17 ± 1	112 ± 8	106 ± 8	470 ± 30	1900 ± 100	14.7 ± 0.8
30	15 ± 1	107 ± 8	107 ± 8	460 ± 30	1800 ± 100	14.3 ± 0.8
40	17 ± 1	127 ± 8	151 ± 8	590 ± 30	2400 ± 100	18.4 ± 0.8
50	29 ± 1	137 ± 8	209 ± 8	750 ± 30	3000 ± 100	23.4 ± 0.8
60	72 ± 1	152 ± 8	254 ± 8	960 ± 30	3800 ± 100	29.9 ± 0.8
65	119 ± 1	173 ± 8	291 ± 8	1170 ± 30	4700 ± 100	36.4 ± 0.8
70	97 ± 1	133 ± 8	203 ± 8	870 ± 30	3500 ± 100	27.0 ± 0.8
80	73 ± 1	103 ± 8	134 ± 8	620 ± 30	2500 ± 100	19.4 ± 0.8
90	34 ± 1	84 ± 8	96 ± 8	430 ± 30	1700 ± 100	13.4 ± 0.8
100	24 ± 1	61 ± 8	72 ± 8	310 ± 30	1300 ± 100	9.8 ± 0.8
110	18 ± 1	59 ± 8	69 ± 8	290 ± 30	1200 ± 100	9.1 ± 0.8
120	16 ± 1	59 ± 8	66 ± 8	280 ± 30	1100 ± 100	8.7 ± 0.8
130	15 ± 1	67 ± 8	67 ± 8	300 ± 30	1200 ± 100	9.3 ± 0.8
140	20 ± 1	87 ± 8	87 ± 8	390 ± 30	1600 ± 100	12.2 ± 0.8

sTable 28. Magnetic state, optimum PTF and enhancement level for the indicated pyradizine resonance relative to that of a single proton

Magnetic state	Optimum PTF / G	Enhancement
Single spin NC**H**	65	284 ± 2
Single spin NCHC**H**	65	238 ± 2
Total single spin order via OPSY	60	750 ± 10
Selective NCHC**H** DQ (SzSz)	50	4.5 ± 0.1
Two spin order between NCHC**H**	30	170 ±5
Three spin order (TQ, eg IzSzS'z)	40, 120	15 ± 2, 21 ± 2
Four spin order (QQ, IzI'zSzS'z)	50, 120	5.97 ± 0.05, 5.06 ± 0.05

sTable 29. Magnetic state, optimum PTF and enhancement level for the indicated phthalazine resonance relative to that of a single proton

Magnetic state	Optimum PTF / G	Enhancement
Single spin NC**H**	65	443 ± 4
Single spin NCHCC**H**	65	37.4 ± 0.2
Single spin NCHCCHC**H**	65	30.5 ± 0.2
Total single spin order via OPSY	65	833 ± 2
Total two spin order via OPSY	65	36.4 ± 0.8

9. SABRE enhancements using 4a and 4b vary with bubbling time

The Solver add-in of Microsoft Excel was used to find a value for the observed rate of polarisation build-up (k_{obs}) by fitting the experimental data to a simulated curve, according to:

$$[B_t] = [B_e] - \frac{[B_e]}{exp^{(k_{obs})t}}$$

Where $[B_t]$ is the concentration of hyperpolarised substrate at time t and $[B_e]$ is the concentration of hyperpolarised substrate at equilibrium.

Pyridazine NC***H*** at 65 G.

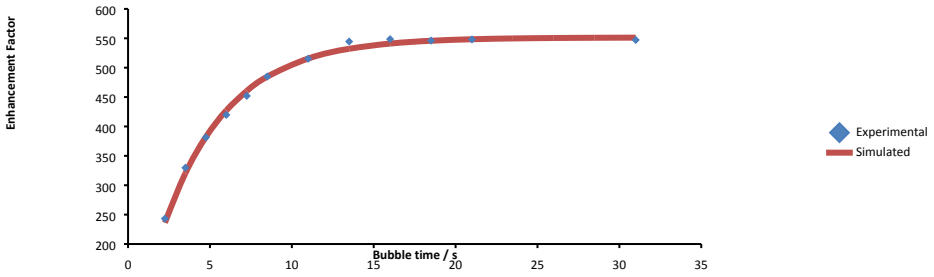

sFigure 13: Scatterplot showing the build-up of polarisation, normalized for the state selection process, at 65 G, for the NC*H* resonance in free pdz, using 4a.

sTable 30: Enhancements in the NC*H* resonance of free pdz using 4a, as a function of bubbling time.

Bubble time / s	Enhancement Factor		Correction for Receiver Gain (/1)
	NC***H***	Total	
1.25	122 ± 2	243 ± 4	243 ± 4
2.5	165 ± 2	330 ± 4	330 ± 4
3.75	191 ± 2	381 ± 4	381 ± 4
5	210 ± 2	420 ± 4	420 ± 4
6.25	226 ± 2	452 ± 4	452 ± 4
7.5	243 ± 2	485 ± 4	485 ± 4
10	258 ± 2	515 ± 4	515 ± 4
12.5	272 ± 2	544 ± 4	544 ± 4
15	274 ± 2	549 ± 4	549 ± 4
17.5	273 ± 2	546 ± 4	546 ± 4
20	274 ± 2	548 ± 4	548 ± 4
30	274 ± 2	547 ± 4	547 ± 4

Pyridazine NCHC***H*** at 65 G.

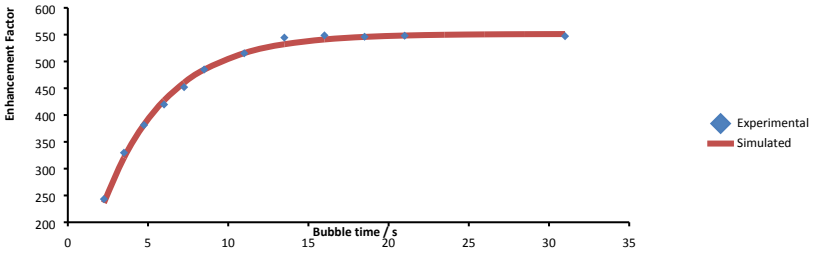

sFigure 14: Scatterplot showing the build-up of polarisation, normalized for the state selection process, at 65 G, for the NCHC*H* resonance free pdz using 4a .

sTable 31: Enhancements in the NCHC*H* resonance of free pdz using 4a, as a function of bubbling time.

Bubble time / s	Enhancement Factor	Correction for Receiver Gain (/1)

	NCHC***H***	Total	
1.25	32 ± 1	63 ± 2	63 ± 2
2.5	49 ± 1	97 ± 2	97 ± 2
3.75	61 ± 1	123 ± 2	123 ± 2
5	68 ± 1	136 ± 2	136 ± 2
6.25	76 ± 1	152 ± 2	152 ± 2
7.5	83 ± 1	165 ± 2	165 ± 2
10	95 ± 1	189 ± 2	189 ± 2
12.5	101 ± 1	203 ± 2	203 ± 2
15	110 ± 1	220 ± 2	220 ± 2
17.5	115 ± 1	229 ± 2	229 ± 2
20	119 ± 1	238 ± 2	238 ± 2
22.5	124 ± 1	248 ± 2	248 ± 2
25	126 ± 1	253 ± 2	253 ± 2
30	130 ± 1	261 ± 2	261 ± 2

Pyridazine NCHC***H***, DQ, at 50 G.

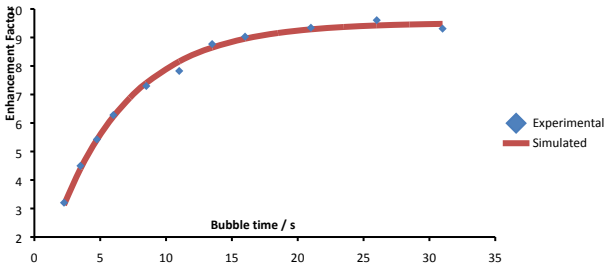

sFigure 15: Scatterplot showing the build-up of polarisation, normalized for the state selection process, at 50 G, for the S_ZS_Z term associated with the two chemically equivalent NCHC*H* resonances in free pdz using 4a.

sTable 32: Enhancements in the NCHC*H* double quantum resonance of free pdz using 4a, as a function of bubbling time.

Bubble time / s	Enhancement Factor		Correction for observation of 1 of 4 terms	Correction for Receiver Gain (/64)
	NCHC***H***	Total		
1.25	26 ± 1	51 ± 2	205 ± 8	3.2 ± 0.1
2.5	36 ± 1	72 ± 2	288 ± 8	4.5 ± 0.1
3.75	43 ± 1	87 ± 2	347 ± 8	5.4 ± 0.1
5	50 ± 1	100 ± 2	402 ± 8	6.3 ± 0.1
7.5	58 ± 1	117 ± 2	467 ± 8	7.3 ± 0.1
10	63 ± 1	125 ± 2	501 ± 8	7.8 ± 0.1
12.5	70 ± 1	140 ± 2	561 ± 8	8.8 ± 0.1
15	72 ± 1	144 ± 2	578 ± 8	9.0 ± 0.1
20	75 ± 1	149 ± 2	598 ± 8	9.3 ± 0.1
25	77 ± 1	154 ± 2	615 ± 8	9.6 ± 0.1
30	74 ± 1	149 ± 2	596 ± 8	9.3 ± 0.1

Pyridazine Single Quantum coherences, at 65 G.

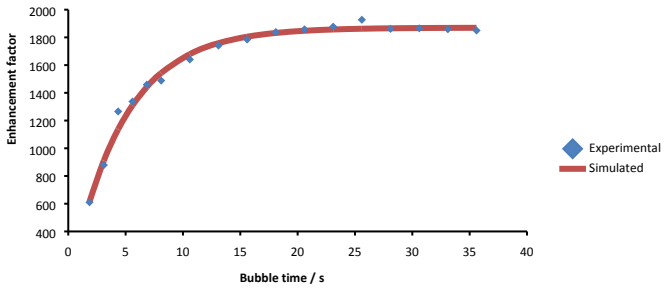

sFigure 16: Scatterplot showing the build-up of polarisation, normalized for the state selection process, at 65 G, for single quantum coherence resonances in free pdz using 4a.

sTable 33: Enhancements in the single quantum coherence resonances of free pdz using 4a, as a function of bubbling time.

Bubble time / s	Enhancement Factor			Correction for observation of 1 of 2 terms	Correction for Receiver Gain (/1)
	NC***H***	NCHC***H***	Total		
1.25	93 ± 2	59 ± 1	305 ± 4	611 ± 8	611 ± 8
2.5	134 ± 2	85 ± 1	439 ± 4	879 ± 8	879 ± 8
3.75	185 ± 2	131 ± 1	632 ± 4	1266 ± 8	1266 ± 8
5	194 ± 2	140 ± 1	669 ± 4	1337 ± 8	1337 ± 8
6.25	212 ± 2	153 ± 1	730 ± 4	1459 ± 8	1459 ± 8
7.5	214 ± 2	158 ± 1	744 ± 4	1488 ± 8	1488 ± 8
10	232 ± 2	179 ± 1	820 ± 4	1641 ± 8	1641 ± 8
12.5	247 ± 2	188 ± 1	870 ± 4	1741 ± 8	1741 ± 8
15	251 ± 2	195 ± 1	893 ± 4	1785 ± 8	1785 ± 8
17.5	256 ± 2	204 ± 1	919 ± 4	1839 ± 8	1839 ± 8
20	262 ± 2	202 ± 1	929 ± 4	1858 ± 8	1858 ± 8
22.5	262 ± 2	207 ± 1	939 ± 4	1877 ± 8	1877 ± 8
25	268 ± 2	214 ± 1	964 ± 4	1927 ± 8	1927 ± 8
27.5	258 ± 2	207 ± 1	931 ± 4	1861 ± 8	1861 ± 8
30	261 ± 2	205 ± 1	933 ± 4	1865 ± 8	1865 ± 8

Pyridazine double quantum coherences, at 30 G.

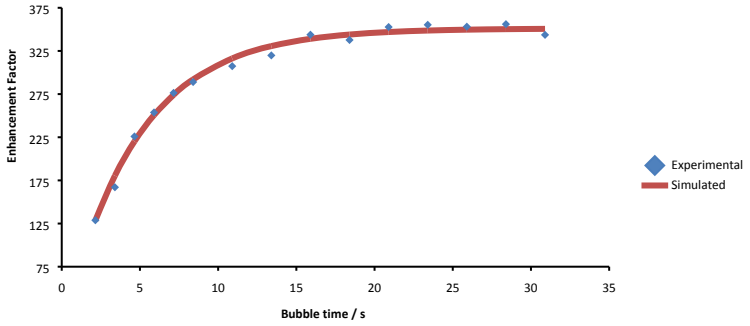

sFigure 17: Scatterplot showing the build-up of polarisation, normalized for the state selection process, at 30 G, for double quantum coherence resonances in free pdz using 4a.

sTable 34: Enhancements in the double quantum coherence resonances of free pdz using 4a, as a function of bubbling time.

Bubble time / s	Enhancement Factor			Correction for observation of 1 of 4 terms	Correction for Receiver Gain (/16)
	NC***H***	NCHC***H***	Total		
1.25	122 ± 6	136 ± 7	520 ± 20	2060 ± 80	129 ± 5
2.5	158 ± 6	176 ± 7	670 ± 20	2670 ± 80	167 ± 5
3.75	214 ± 6	238 ± 7	900 ± 20	3620 ± 80	226 ± 5
5	239 ± 6	268 ± 7	1010 ± 20	4060 ± 80	254 ± 5
6.25	261 ± 6	292 ± 7	1110 ± 20	4420 ± 80	276 ± 5
7.5	273 ± 6	305 ± 7	1160 ± 20	4620 ± 80	289 ± 5
10	290 ± 6	325 ± 7	1230 ± 20	4920 ± 80	307 ± 5
12.5	302 ± 6	338 ± 7	1280 ± 20	5120 ± 80	320 ± 5
15	325 ± 6	363 ± 7	1380 ± 20	5500 ± 80	344 ± 5
17.5	319 ± 6	357 ± 7	1350 ± 20	5400 ± 80	338 ± 5
20	333 ± 6	372 ± 7	1410 ± 20	5640 ± 80	353 ± 5
22.5	335 ± 6	375 ± 7	1420 ± 20	5690 ± 80	355 ± 5
25	334 ± 6	373 ± 7	1410 ± 20	5650 ± 80	353 ± 5
27.5	336 ± 6	376 ± 7	1420 ± 20	5700 ± 80	356 ± 5
30	325 ± 6	362 ± 7	1370 ± 20	5500 ± 80	344 ± 5

Pyridazine triple quantum coherences, at 120 G.

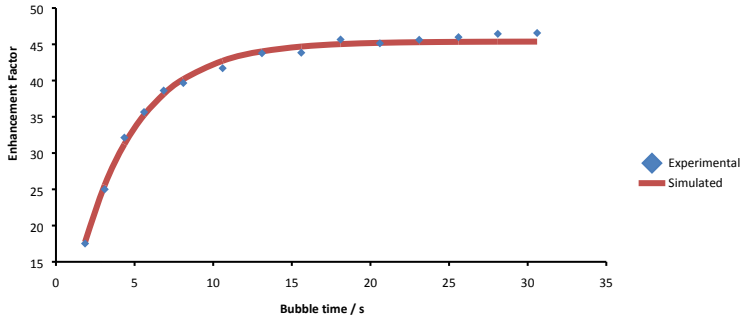

sFigure 18: Scatterplot showing the build-up of polarisation, normalized for the state selection process, at 120 G, for triple quantum coherence resonances in free pdz using 4a.

sTable 35: Enhancements in the triple quantum coherence resonances of free pdz using 4a, as a function of bubbling time.

Bubble time / s	Enhancement Factor			Correction for observation of 1 of 8 terms	Correction for Receiver Gain (/114)
	NC***H***	NCHC***H***	Total		
1.25	80 ± 10	40 ± 10	250 ± 30	2000 ± 200	18 ± 2
2.5	120 ± 10	60 ± 10	360 ± 30	2900 ± 200	25 ± 2
3.75	150 ± 10	80 ± 10	460 ± 30	3700 ± 200	32 ± 2
5	160 ± 10	90 ± 10	510 ± 30	4100 ± 200	36 ± 2
6.25	180 ± 10	100 ± 10	550 ± 30	4400 ± 200	39 ± 2
7.5	180 ± 10	100 ± 10	570 ± 30	4500 ± 200	40 ± 2
10	180 ± 10	110 ± 10	590 ± 30	4800 ± 200	42 ± 2
12.5	200 ± 10	120 ± 10	620 ± 30	5000 ± 200	44 ± 2
15	200 ± 10	120 ± 10	620 ± 30	5000 ± 200	44 ± 2
17.5	200 ± 10	120 ± 10	650 ± 30	5200 ± 200	46 ± 2
20	200 ± 10	120 ± 10	640 ± 30	5100 ± 200	45 ± 2
22.5	200 ± 10	120 ± 10	650 ± 30	5200 ± 200	46 ± 2
25	200 ± 10	130 ± 10	660 ± 30	5200 ± 200	46 ± 2
27.5	210 ± 10	130 ± 10	660 ± 30	5300 ± 200	46 ± 2
30	200 ± 10	130 ± 10	660 ± 30	5300 ± 200	47 ± 2

Pyridazine quadruple quantum coherences, at 50 G.

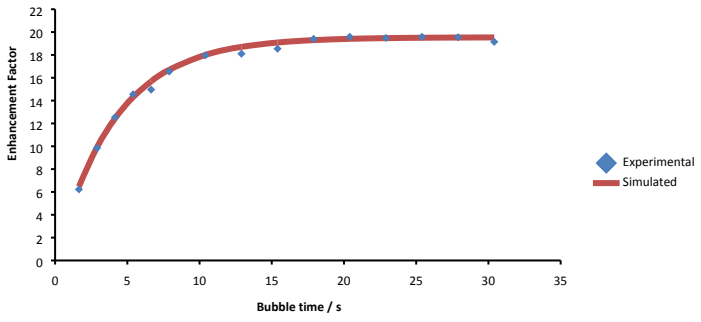

sFigure 19: Scatterplot showing the build-up of polarisation, normalized for the state selection process, at 50 G, for quadruple quantum coherence resonances in free pdz using 4a.

sTable 36: Enhancements in the quadruple quantum coherence resonances of free pdz using 4a, as a function of bubbling time.

Bubble time / s	Enhancement Factor			Correction for observation of 1 of 16 terms	Correction for Receiver Gain (/2050)
	NC***H***	NCHC***H***	Total		

1.25	170 ± 10	230 ± 10	800 ± 30	12800 ± 500	6.2 ± 0.2
2.5	270 ± 10	370 ± 10	1260 ± 30	20200 ± 500	9.8 ± 0.2
3.75	340 ± 10	470 ± 10	1610 ± 30	25700 ± 500	12.5 ± 0.2
5	380 ± 10	550 ± 10	1860 ± 30	29800 ± 500	14.5 ± 0.2
6.25	400 ± 10	560 ± 10	1920 ± 30	30700 ± 500	15.0 ± 0.2
7.5	450 ± 10	620 ± 10	2120 ± 30	33900 ± 500	16.6 ± 0.2
10	480 ± 10	670 ± 10	2300 ± 30	36800 ± 500	18.0 ± 0.2
12.5	490 ± 10	670 ± 10	2320 ± 30	37100 ± 500	18.1 ± 0.2
15	490 ± 10	700 ± 10	2380 ± 30	38000 ± 500	18.5 ± 0.2
17.5	510 ± 10	730 ± 10	2490 ± 30	39800 ± 500	19.4 ± 0.2
20	520 ± 10	730 ± 10	2510 ± 30	40200 ± 500	19.6 ± 0.2
22.5	520 ± 10	730 ± 10	2500 ± 30	40000 ± 500	19.5 ± 0.2
25	520 ± 10	730 ± 10	2510 ± 30	40200 ± 500	19.6 ± 0.2
27.5	520 ± 10	730 ± 10	2510 ± 30	40100 ± 500	19.5 ± 0.2
30	520 ± 10	710 ± 10	2500 ± 30	39300 ± 500	19.1 ± 0.2

Summary:

sTable 37: Rate constants of the build-up of polarisation with bubbling time into the magnetic states of free pdz using 4a.

Magnetic states	k_{obs} of polarisation build-up / s^{-1}
I_z	0.249 ± 0.007
S_z	0.122 ± 0.005
S_zS_z	0.177 ± 0.005
SQ	0.215 ± 0.007
DQ	0.212 ± 0.006
TQ	0.268 ± 0.007
QQ	0.244 ± 0.005

Phthalazine NC***H***, at 65 G.

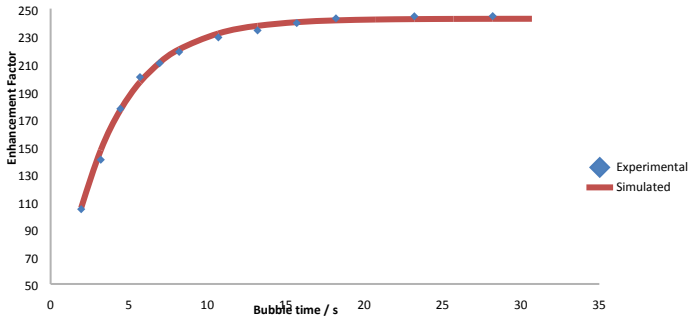

sFigure 20: Scatterplot showing the build-up of polarisation, normalized for the state selection process, at 65 G, for the NC*H* resonance in free phth using 4b.

sTable 38: Enhancements in the NC*H* resonances of free phth using 4b, as a function of bubbling time.

Bubble time / s	Enhancement Factor		Correction for Receiver Gain (/1)
	NC***H***	Total	
1.25	52 ± 1	104 ± 2	104 ± 2
2.5	70 ± 1	140 ± 2	140 ± 2
3.75	89 ± 1	177 ± 2	177 ± 2
5	100 ± 1	200 ± 2	200 ± 2
6.25	105 ± 1	210 ± 2	210 ± 2
7.5	109 ± 1	219 ± 2	219 ± 2
10	115 ± 1	229 ± 2	229 ± 2
12.5	117 ± 1	234 ± 2	234 ± 2
15	120 ± 1	240 ± 2	240 ± 2
17.5	121 ± 1	243 ± 2	243 ± 2
22.5	122 ± 1	244 ± 2	244 ± 2

27.5	122 ± 1	245 ± 2	245 ± 2

Phthalazine NCHCC***H***, at 65 G.

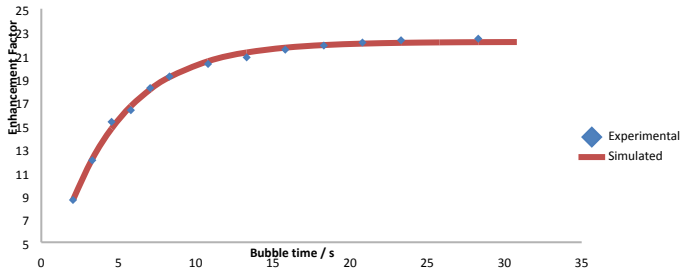

sFigure 21: Scatterplot showing the build-up of polarisation, normalized for the state selection process, at 65 G, for the NCHCC*H* resonance in free phth using 4b.

sTable 39: Enhancements in the NCHCC*H* resonances of free phth using 4b, as a function of bubbling time.

Bubble time / s	Enhancement Factor		Correction for Receiver Gain (/16)
	NCHCC***H***	Total	
1.25	69 ± 2	138 ± 4	8.6 ± 0.2
2.5	96 ± 2	192 ± 4	12.0 ± 0.2
3.75	123 ± 2	245 ± 4	15.3 ± 0.2
5	130 ± 2	261 ± 4	16.3 ± 0.2
6.25	146 ± 2	291 ± 4	18.2 ± 0.2
7.5	154 ± 2	307 ± 4	19.2 ± 0.2
10	162 ± 2	324 ± 4	20.3 ± 0.2
12.5	167 ± 2	333 ± 4	20.8 ± 0.2
15	172 ± 2	344 ± 4	21.5 ± 0.2
17.5	175 ± 2	350 ± 4	21.8 ± 0.2
20	177 ± 2	354 ± 4	22.1 ± 0.2
22.5	178 ± 2	357 ± 4	22.3 ± 0.2
27.5	180 ± 2	359 ± 4	22.4 ± 0.2

Phthalazine NCHCCHC***H***, at 65 G.

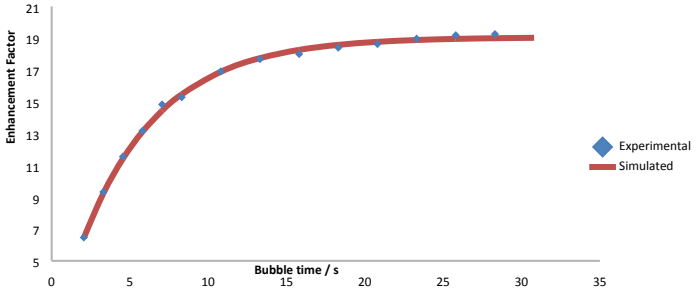

sFigure 21: Scatterplot showing the build-up of polarisation, normalized for the state selection process, at 65 G, for the NCHCCHC*H* resonance in free phth using 4b.

sTable 40: Enhancements in the NCHCCHC*H* resonances of free phth using 4b, as a function of bubbling time.

Bubble time / s	Enhancement Factor		Correction for Receiver Gain (/16)
	NCHCCHC***H***	Total	
1.25	51.7 ± 0.7	103 ± 1	6.47 ± 0.06
2.5	74.6 ± 0.7	149 ± 1	9.33 ± 0.06
3.75	92.4 ± 0.7	185 ± 1	11.55 ± 0.06
5	105.4 ± 0.7	211 ± 1	13.18 ± 0.06
6.25	118.7 ± 0.7	237 ± 1	14.83 ± 0.06

7.5	122.3 ± 0.7	245 ± 1	15.29 ± 0.06
10	135.3 ± 0.7	271 ± 1	16.91 ± 0.06
12.5	141.5 ± 0.7	283 ± 1	17.68 ± 0.06
15	144.0 ± 0.7	288 ± 1	18.00 ± 0.06
17.5	147.2 ± 0.7	294 ± 1	18.40 ± 0.06
20	149.0 ± 0.7	298 ± 1	18.63 ± 0.06
22.5	151.8 ± 0.7	304 ± 1	18.97 ± 0.06
25	153.5 ± 0.7	307 ± 1	19.18 ± 0.06
27.5	154.0 ± 0.7	308 ± 1	19.26 ± 0.06

Phthalazine Single quantum coherences

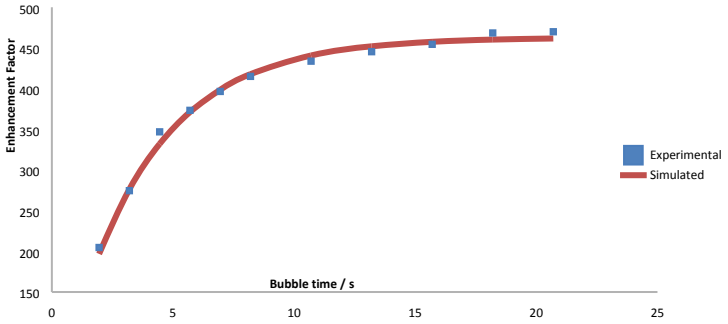

sFigure 22: Scatterplot showing the build-up of polarisation, normalized for the state selection process, at 65 G, for single quantum coherence resonances in free phth using 4b.

sTable 41: Enhancements in the single quantum coherence resonances of free phth using 4b, as a function of bubbling time.

Bubble time / s	Enhancement Factor				Correction for detection of 1 of 2 terms	Correction for Receiver Gain (/4)
	NC***H***	NCHCC***H***	NCHCCHC***H***	Total		
1.25	155 ± 3	29.7 ± 0.7	20.2 ± 0.5	409 ± 6	820 ± 10	205 ± 2
2.5	205 ± 3	40.9 ± 0.7	28.3 ± 0.5	549 ± 6	1100 ± 10	275 ± 2
3.75	256 ± 3	53.3 ± 0.7	37.5 ± 0.5	694 ± 6	1390 ± 10	347 ± 2
5	274 ± 3	58.0 ± 0.7	41.7 ± 0.5	747 ± 6	1490 ± 10	373 ± 2
6.25	289 ± 3	62.1 ± 0.7	45.4 ± 0.5	793 ± 6	1590 ± 10	397 ± 2
7.5	301 ± 3	65.7 ± 0.7	48.4 ± 0.5	830 ± 6	1660 ± 10	415 ± 2
10	312 ± 3	69.6 ± 0.7	52.1 ± 0.5	867 ± 6	1730 ± 10	434 ± 2
12.5	319 ± 3	71.7 ± 0.7	54.6 ± 0.5	890 ± 6	1780 ± 10	445 ± 2
15	324 ± 3	73.8 ± 0.7	56.6 ± 0.5	909 ± 6	1820 ± 10	455 ± 2
17.5	333 ± 3	76.3 ± 0.7	59.1 ± 0.5	937 ± 6	1870 ± 10	468 ± 2
20	334 ± 3	76.7 ± 0.7	59.6 ± 0.5	940 ± 6	1880 ± 10	470 ± 2

Phthalazine double quantum coherences, at 65 G.

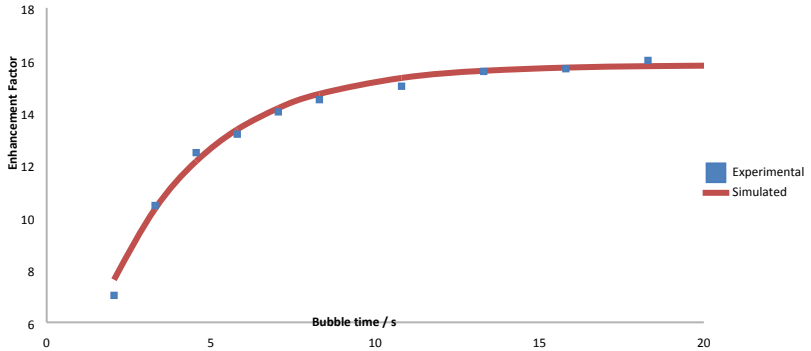

sFigure 23: Scatterplot showing the build-up of polarisation, normalized for the state selection process, at 65 G, for double quantum coherence resonances in free phth using 4b.

sTable 42: Enhancements in the double quantum coherence resonances of free phth using 4b, as a function of bubbling time.

Bubble time / s	Enhancement Factor				Correction for detection of 1 of 4 terms	Correction for Receiver Gain (/128)
	NC***H***	NCHCC***H***	NCHCCHC***H***	Total		
1.25	20 ± 2	38 ± 2	55 ± 4	220 ± 10	900 ± 40	7.0 ± 0.3
2.5	33 ± 2	53 ± 2	81 ± 4	330 ± 10	1340 ± 40	10.5 ± 0.3
3.75	41 ± 2	63 ± 2	96 ± 4	400 ± 10	1600 ± 40	12.5 ± 0.3
5	44 ± 2	65 ± 2	102 ± 4	420 ± 10	1690 ± 40	13.2 ± 0.3
6.25	49 ± 2	68 ± 2	108 ± 4	450 ± 10	1800 ± 40	14.0 ± 0.3
7.5	51 ± 2	70 ± 2	111 ± 4	460 ± 10	1860 ± 40	14.5 ± 0.3
10	54 ± 2	72 ± 2	114 ± 4	480 ± 10	1920 ± 40	15.0 ± 0.3
12.5	56 ± 2	74 ± 2	119 ± 4	500 ± 10	2000 ± 40	15.6 ± 0.3
15	56 ± 2	75 ± 2	120 ± 4	500 ± 10	2010 ± 40	15.7 ± 0.3
17.5	58 ± 2	76 ± 2	122 ± 4	510 ± 10	2050 ± 40	16.0 ± 0.3
20	59 ± 2	76 ± 2	123 ± 4	520 ± 10	2060 ± 40	16.1 ± 0.3

Summary:

Table 43: Rate constants of the build-up of polarisation with bubbling time into the magnetic states of free phth using 4b.

Magnetic states	k_{obs} of polarisation build-up / s^{-1}
I_z	0.292 ± 0.006
S_z	0.240 ± 0.006
T_z	0.201 ± 0.003
SQ	0.28 ± 0.01
DQ	0.32 ± 0.01

10. Calculation of T_1 values for magnetic states in pyridazine and phthalazine

A 2-D inversion recovery experiment was collected to calculate the T_1 values of single quantum terms. The intensity of the signals at a given time were calculated and plotted. The signal intensity is proportional to the T_1 values according to:

$$M_\tau = M_0[1 - 2exp^{\frac{-\tau}{T_1}}]$$

Where M_τ is the magnetisation (measured using the integrals) after a delay of time τ, and M_0 is the magnetisation after a delay of time $\tau >> T_1$. Solver was used to simulate the data, by minimising the root mean square between calculated data and experimental data, by allowing the T_1 and M_0 values to change. The results are shown in the table and the plots below.

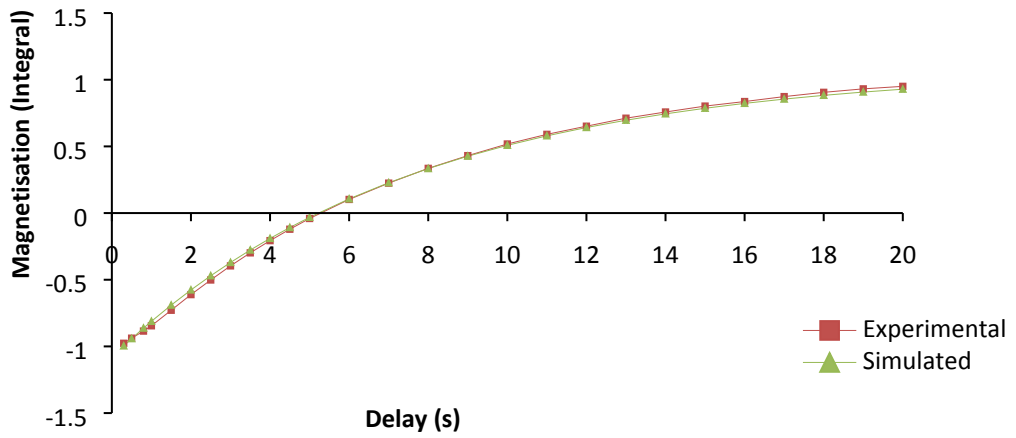

sFigure 24: Plot to show the intensity of free pyridazine signal δ 9.28 as a function of time in an inversion recovery experiment.

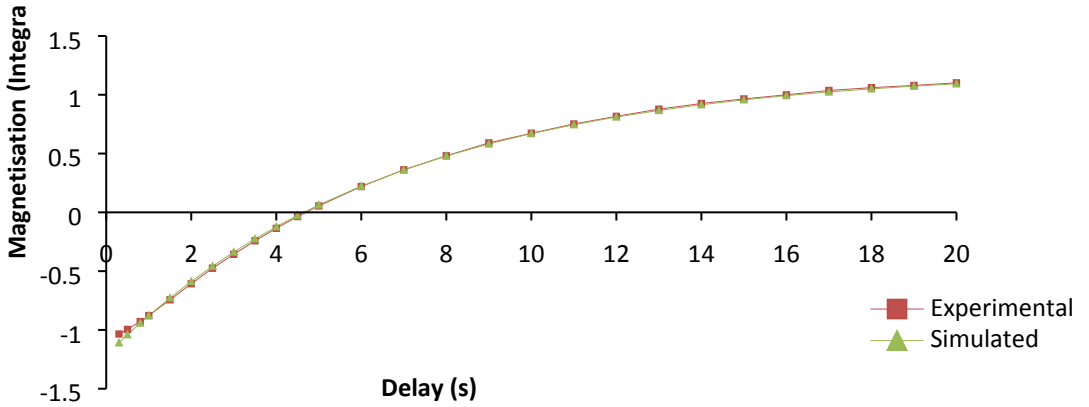

sFigure 25: Plot to show the intensity of free pyridazine signal δ 7.78 as a function of time in an inversion recovery experiment.

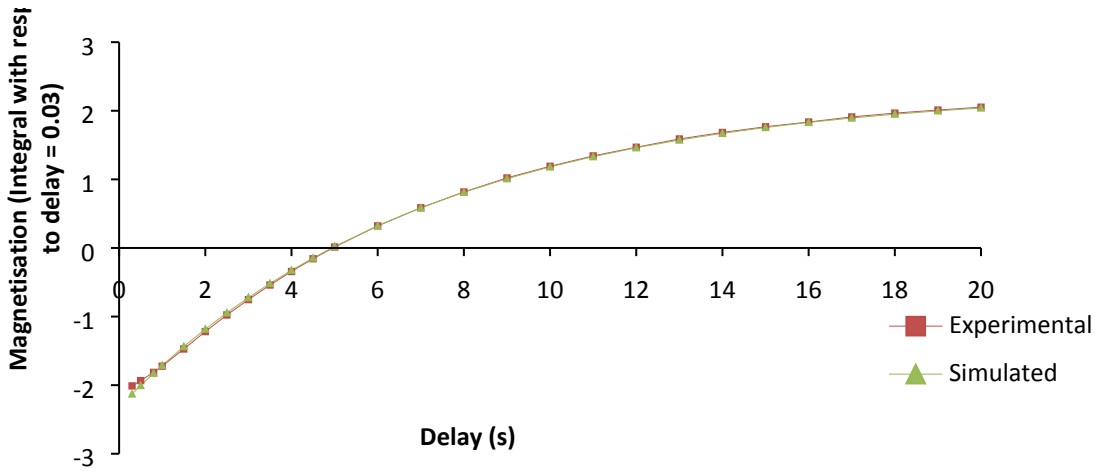

sFigure 26: Plot to show the intensity of the sum of the free pyridazine signals as a function of time in an inversion recovery experiment.

sTable 44: The calculated T_1 values for specific magnetic states of pyridazine.

^{1}H NMR Signal	T_1 (s)	M_0
9.28	7.613 ± 0.001	1.08
7.78	6.697 ± 0.001	1.22
SQ	7.118 ± 0.001	2.32

The T_1 value of the double quantum H_BH_B' signal was also calculated by selectively creating the state and then collecting ^{1}H NMR spectra after specific, set times. The data was fitted to the formula below (this is slightly different as it is not an inversion recovery experiment):

$$M_\tau = M_0[2exp^{\frac{-\tau}{T_1}}]$$

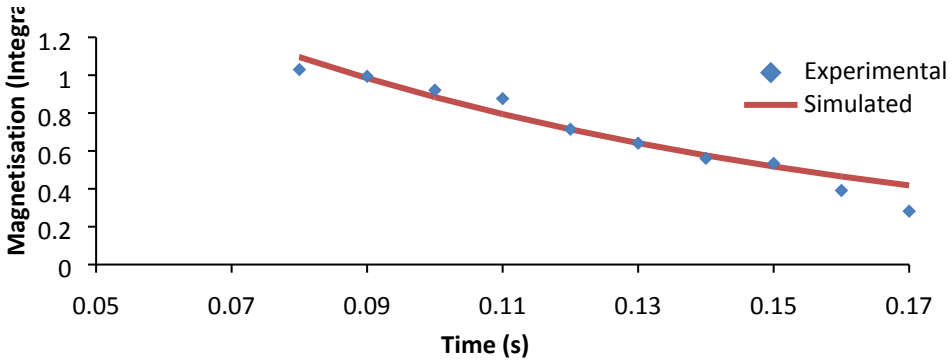

sFigure 27: Plot to show the intensity of the double quantum H_BH_B' free pyridazine signal at δ 7.78 as a function of time in an inversion recovery experiment.

The T_1 value calculated from this fitting is 0.086 s ± 0.001 s, which is far quicker than the other states. The rate of polarisation build-up can now be corrected for the T_1 relaxation:

sTable 45: The calculated rates of polarisation build-up for specific magnetic states of pyridazine.

State probed	Rate of polarisation build-up / s^{-1}
I_z	0.380 ± 0.007
S_z	0.271 ± 0.005
S_zS_z	11.79 ± 0.005
SQ	0.356 ± 0.007
DQ	12.94 ± 0.006

Although the double quantum states relax much more quickly than the single quantum, they polarise much more quickly and this counteracts the relaxation, allowing the states to become populated.

The same 2-D inversion recovery experiment was collected for the analogous phthalazine sample. The results are shown in the table and the plots below:

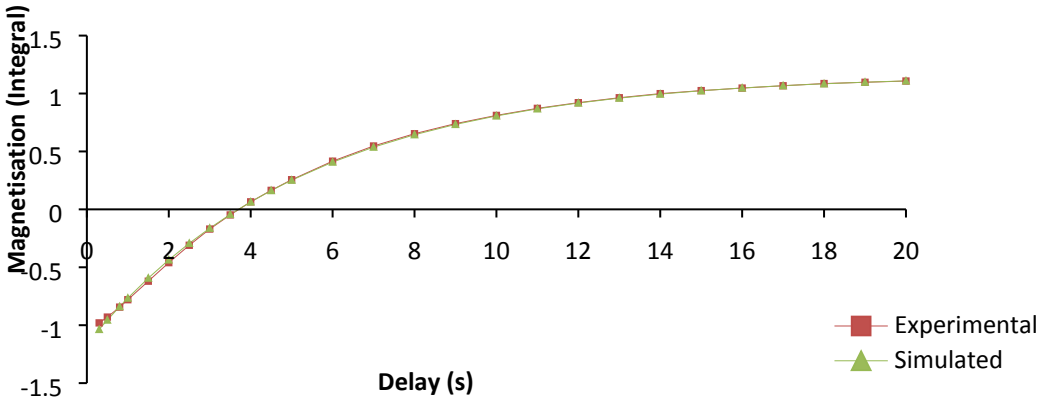

sFigure 28: Plot to show the intensity of the phthalazine signal at δ 9.64 as a function of time in an inversion recovery experiment.

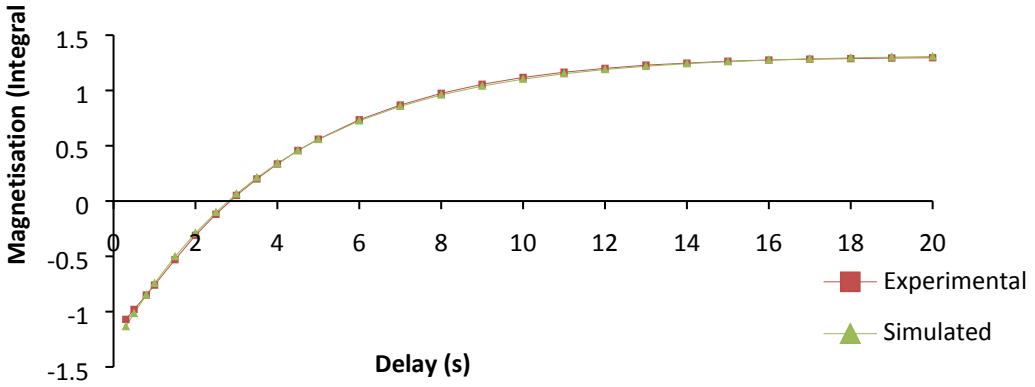

sFigure 29: Plot to show the intensity of the phthalazine signal at δ 8.20 as a function of time in an inversion recovery experiment.

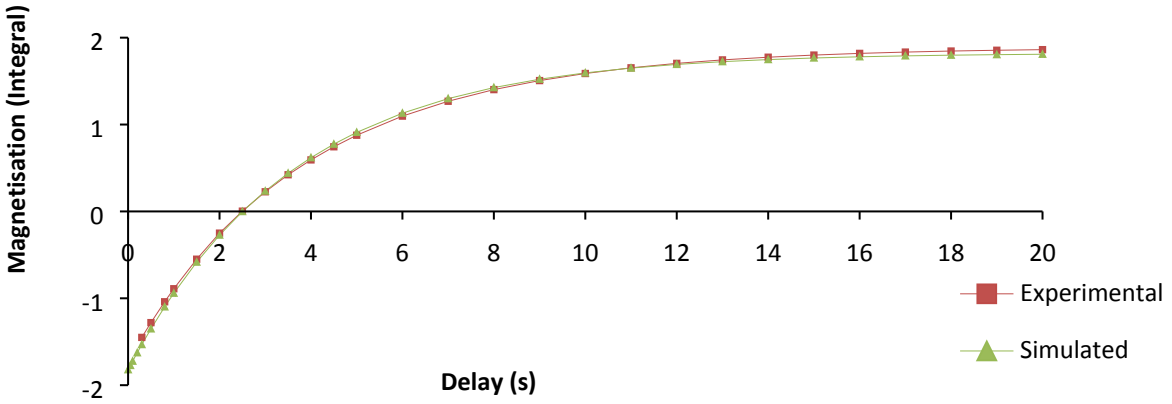

sFigure 30: Plot to show the intensity of the phthalazine signal at δ 8.10 as a function of time in an inversion recovery experiment.

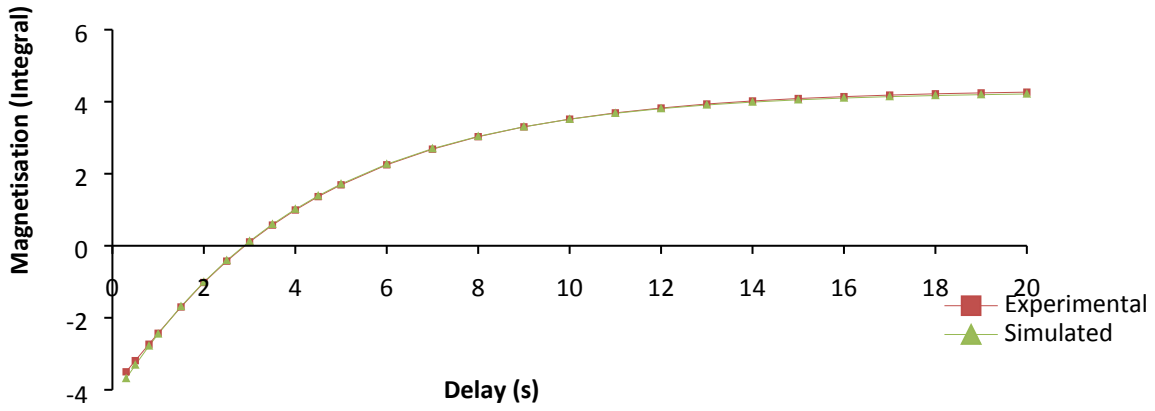

sFigure 31: Plot to show the intensity of the sum of the free phthalazine signals as a function of time in an inversion recovery experiment.

sTable 46: The calculated T_1 values for specific magnetic states of phthalazine.

^{1}H NMR Signal	T_1 (s)	M_0
9.64	5.335 ± 0.001	1.16
8.20	4.0375 ± 0.0009	1.32
8.10	3.6153 ± 0.0007	1.83
SQ	4.1523 ± 0.0007	4.29

The rate of polarisation build-up can now be corrected for the T_1 relaxation.

sTable 47: The calculated rates of polarisation build-up for specific magnetic states of phthalazine.

State probed	Rate of polarisation build-up / s^{-1}
$\mathbf{I_z}$	0.477 ± 0.006
$\mathbf{S_z}$	0.488 ± 0.006
$\mathbf{T_z}$	0.476 ± 0.003
SQ	0.52 ± 0.01

11. Model for ligand exchange in 4a and 4b

The pathways available to transfer polarisation from a selectively-excited IrNNC**H** proton to an IrNC**H** or free NC**H** proton are shown below, where K_a is the rate of association, K_d is the rate of dissociation, and K_h is the rate of the haptotropic shift.

sScheme 2: Exchange pathways available to an IrNNC*H* proton.

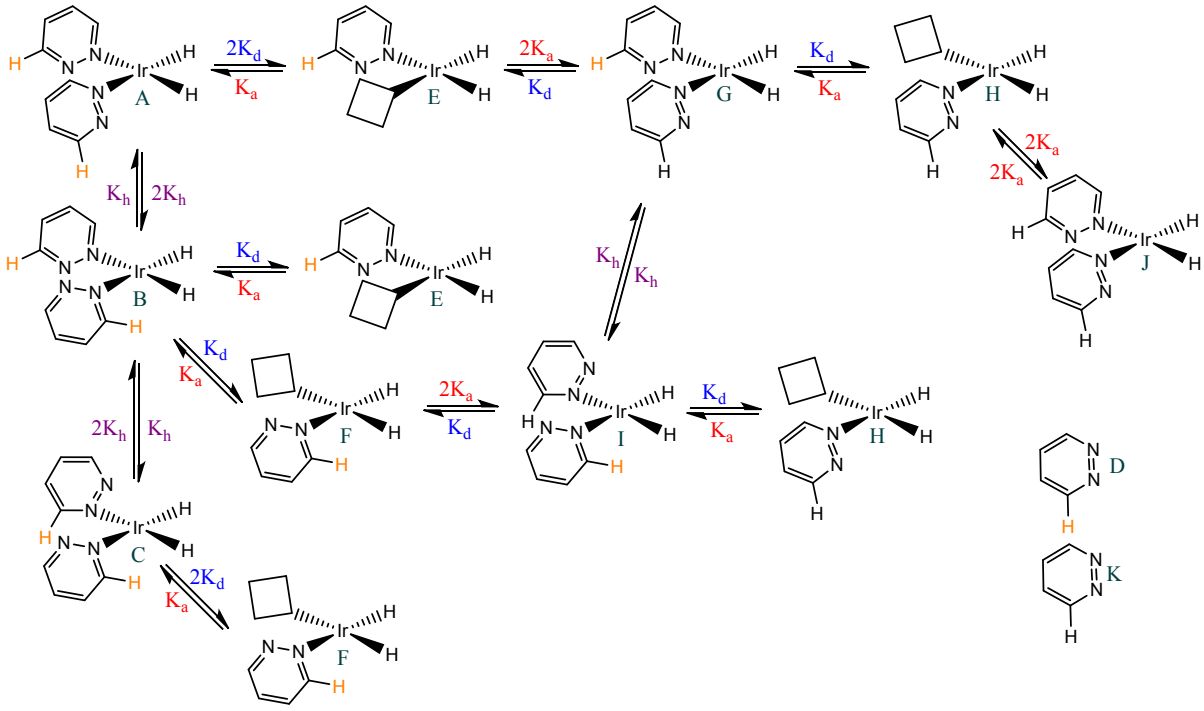

The concentration of each species, after time t, can be calculated from the formulae shown:

$$[A]_t = [A]_0 - (2K_d[A])t + (K_a[E][D])t + (K_h[B])t$$

$$[B]_t = [B]_0 - (2K_h[B])t - (2K_d[B])t + (2K_h[A])t + (2K_h[C])t + (K_a[E][D])t + (K_a[F][D])t$$

$$[C]_t = [C]_0 - (2K_h[C])t - (2K_d[C])t + (K_h[B])t + (K_a[F][D])t$$

$$[D]_t = [D]_0 - (2K_a[E][D])t - 2K_a[F][D])t - (2K_a[H][D])t + (2K_d[A])t + (2K_d[B])t + + (K_d[I])t$$

$$[E]_t = [E]_0 - (2K_a[E][K])t - (2K_a[E][D]) + (2K_d[A])t + (K_d[G])t + (K_d[B])t$$

$$[F]_t = [F]_0 - (2K_a[F][K])t - (2K_a[F][D])t + (2K_d[C])t + (K_d[B])t + (K_d[I])t$$

$$[G]_t = [G]_0 - (2K_d[G])t - (K_h[G])t + (2K_a[E][K])t + (K_a[H][D])t + (K_h[I])t$$

$$[H]_t = [H]_0 - (2K_a[H][D])t - (2K_a[H][K])t + (K_d[G])t + (K_d[I])t + (2K_d[J])t$$

$$[I]_t = [I]_0 - (2K_d[I])t - (K_h[I])t + (K_a[H][D])t + (2K_a[F][K])t + (K_h[G])t$$

$$[J]_t = [J]_0 - (2K_d[J])t + (2K_a[H][K])t$$

$$[K]_t = [K]_0 - (2K_a[E][K])t - (2K_a[F][K])t - (2K_a[H][K])t + (2K_d[J])t + (2K_d[G])t + (K_d[I])t$$

Microsoft Excel's Solver was used to simulate the data, by minimising the root mean square between calculated data and experimental data, by allowing the K_a, K_d, and K_h values to change.

12. Useful ^{1}H NMR spectra

2a with free pdz(*), methanol-d_4, 500 MHz

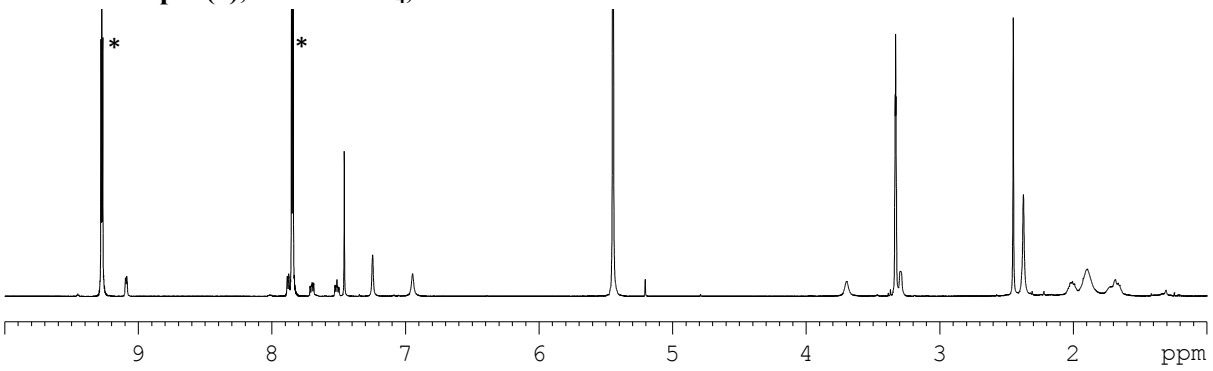

2b with free phth (*),methanol-d_4, 500 MHz

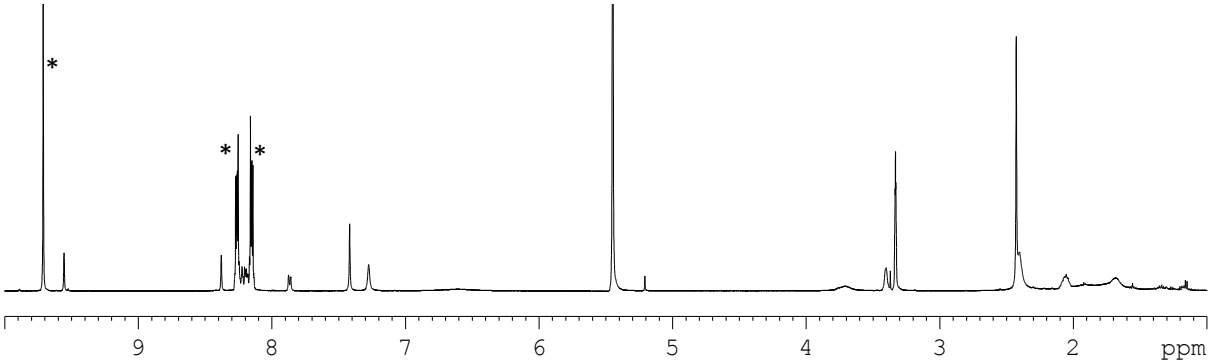

3a with free pdz(*), methanol-d_4, 500 MHz

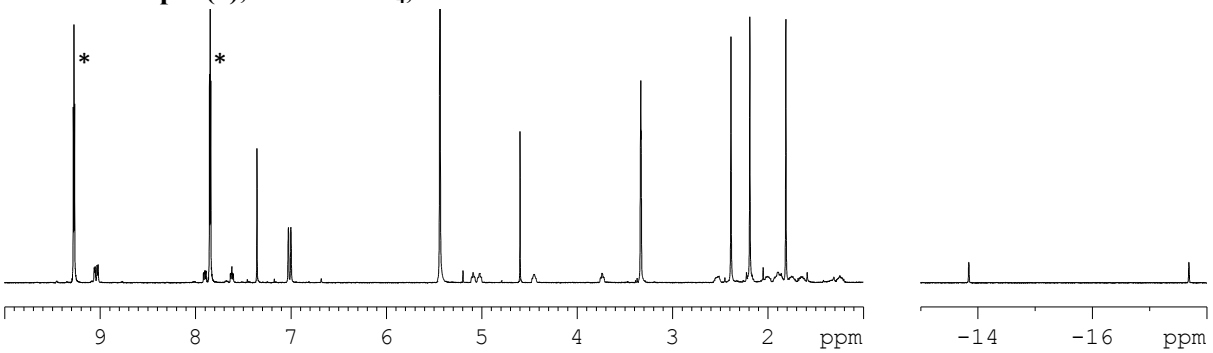

3b with free phth(*), methanol-d_4, 500 MHz

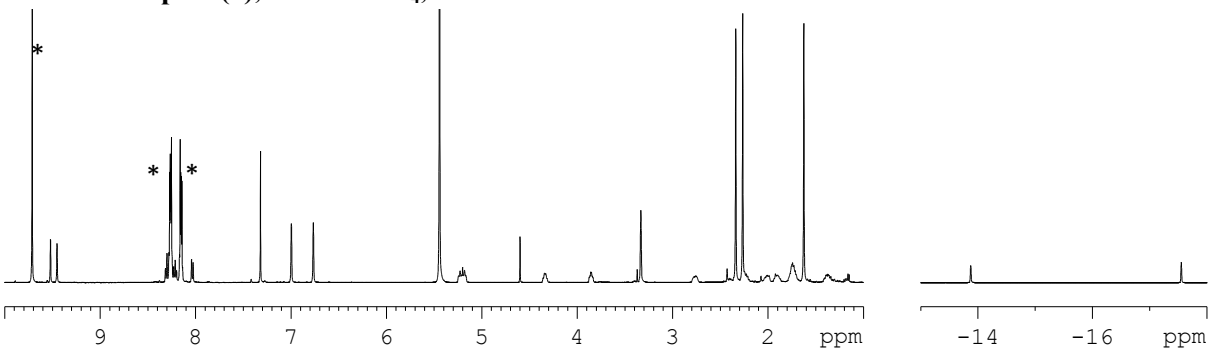

4a with free pdz(*), methanol-d_4, 500 MHz

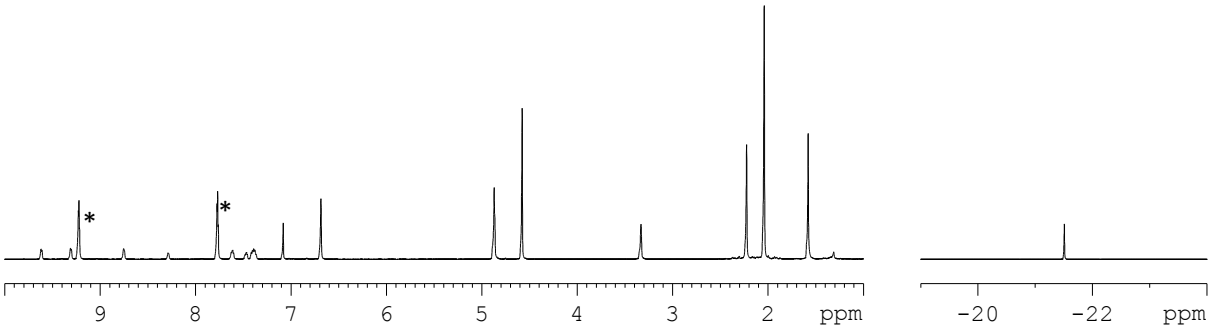

4b with free phth(*), methanol-d_4, 500 MHz

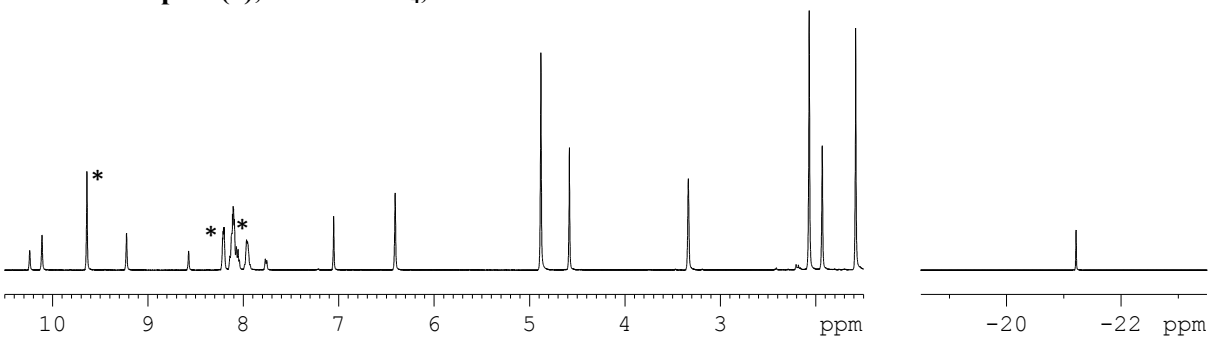

4a with free pdz(*), methanol-d_4, 500 MHz, polarised by SABRE

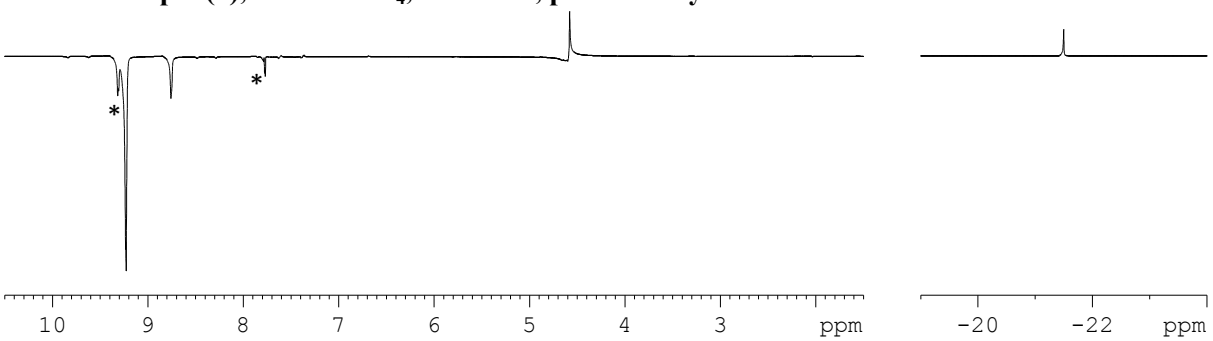

4b with free phth(*), methanol-d_4, 500 MHz, polarised by SABRE

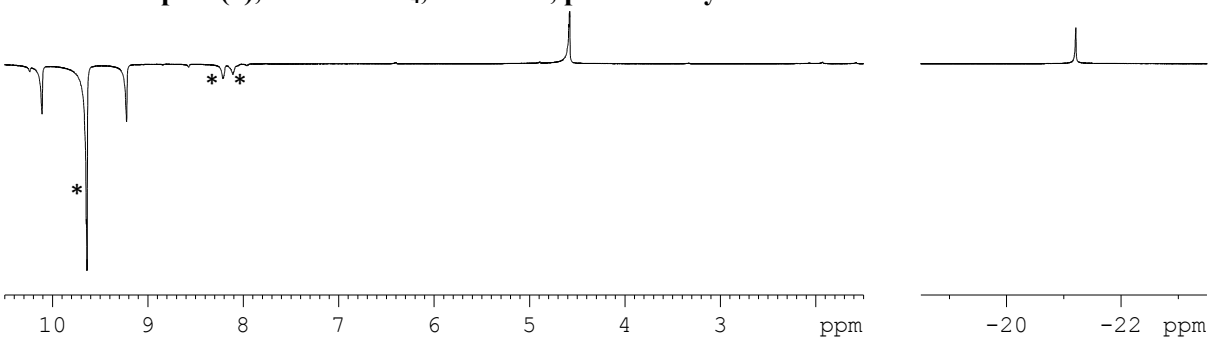

4a with free pdz(*), ethanol-d_6, 400 MHz, polarised by SABRE

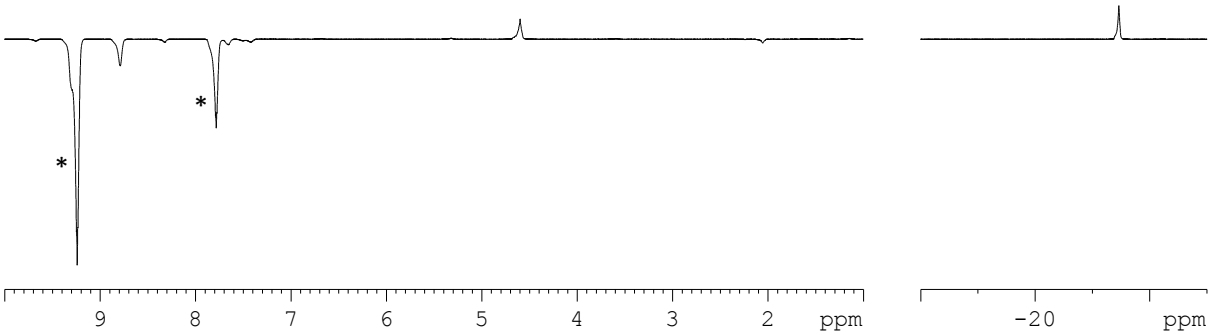

4b with free phth(*), ethanol-d_6, 400 MHz, polarised by SABRE

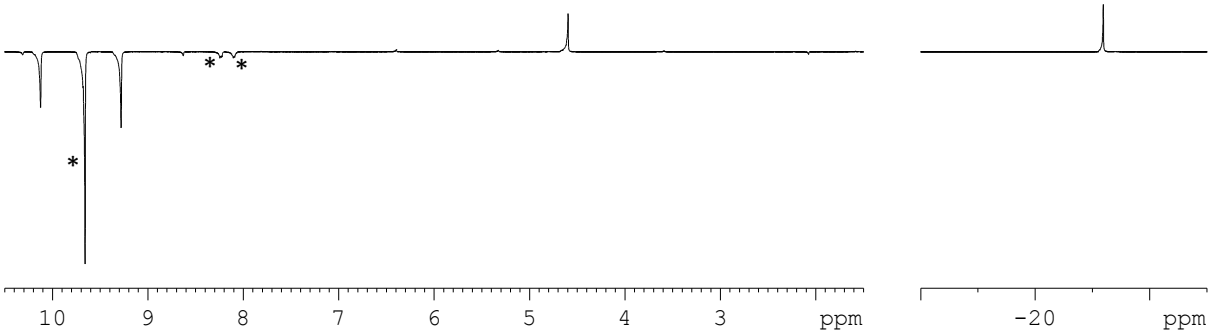

Polarisation of 5-aminophthalazine (*) by SABRE with 1 and *p*-H_2, methanol-d_6, 400 MHz